

Dynamic Time Warping based Adversarial Framework for Time-Series Domain

Taha Belkhouja, Yan Yan, *Member, IEEE* and Janardhan Rao Doppa, *Member, IEEE*

Abstract—Despite the rapid progress on research in adversarial robustness of deep neural networks (DNNs), there is little principled work for the time-series domain. Since time-series data arises in diverse applications including mobile health, finance, and smart grid, it is important to verify and improve the robustness of DNNs for the time-series domain. In this paper, we propose a novel framework for the time-series domain referred as *Dynamic Time Warping for Adversarial Robustness (DTW-AR)* using the dynamic time warping measure. Theoretical and empirical evidence is provided to demonstrate the effectiveness of DTW over the standard Euclidean distance metric employed in prior methods for the image domain. We develop a principled algorithm justified by theoretical analysis to efficiently create diverse adversarial examples using random alignment paths. Experiments on diverse real-world benchmarks show the effectiveness of DTW-AR to fool DNNs for time-series data and to improve their robustness using adversarial training. The source code of DTW-AR algorithms is available at <https://github.com/tahabelkhouja/DTW-AR>

Index Terms—Time Series, Robustness, Deep Neural Networks, Adversarial Examples, Dynamic Time Warping.



1 INTRODUCTION

TO deploy deep neural network (DNN) based systems in important real-world applications such as healthcare, we need them to be robust. Adversarial methods expose the brittleness of DNNs and motivate methods to improve their robustness. There is little principled work for the time-series domain even though this type of data arises in many real-world applications including mobile health [1], finance [2], and smart grid analytics [3]. The time-series modality poses unique challenges for studying adversarial robustness that are not seen in images [4] and text [5]. The standard approach of imposing an l_p -norm bound to create worst possible scenarios from a learning agent's perspective doesn't capture the true similarity between time-series instances. Consequently, l_p -norm constrained perturbations can potentially create adversarial examples that correspond to a completely different class label. There is no prior work on filtering methods in the signal processing literature to *automatically* identify such adversarial candidates. Hence, adversarial examples from prior methods based on l_p -norm will confuse the learner when they are used to improve the robustness of DNNs. In other words, the accuracy of DNNs will degrade on real-world data after adversarial training.

This paper proposes a novel adversarial framework for time-series domain referred as *Dynamic Time Warping for Adversarial Robustness (DTW-AR)* to address the above-mentioned challenges. DTW-AR employs the dynamic time warping measure [6], [7] as it can be used to measure a realistic distance between two time-series signals (e.g., invariance to shift and scaling operations) [7], [8]. For example, a signal that has its frequency changed due to Doppler effect would output a small DTW measure to the original signal. However, if Euclidean distance is used, both signals would look very dissimilar, unlike the reality. We theoretically analyze the

suitability of DTW measure over the Euclidean distance. Specifically, the space of candidate adversarial examples in the DTW space is a superset of those in Euclidean space for the same distance bound. Therefore, DTW measure provides a more appropriate bias than the Euclidean space for the time series domain and our experiments demonstrate practical benefits of DTW-based adversarial examples.

To create targeted adversarial examples, we formulate an optimization problem with the DTW measure bound constraint and propose to solve it using an iterative gradient-based approach. However, this simple method has two drawbacks. First, this method allows us to only find one valid adversarial example out of multiple solution candidates from the search space because it operates on a single optimal alignment. Second, we need to compute DTW measure in each iteration as the optimal DTW alignment path changes over iterations. Since the number of iterations are typically large and DTW computation is expensive, the overall algorithm becomes prohibitively slow. To successfully overcome these two drawbacks, *our key insight is to employ stochastic alignments to create adversarial examples*. We theoretically and experimentally show that a simpler distance measure based on random alignment path upper-bounds the DTW measure and that this *bound is tight*. This algorithm allows us to efficiently create many diverse adversarial examples using different alignment paths to improve the robustness of DNN models via adversarial training. Our experiments on real-world time-series datasets show that the DTW-AR creates more effective adversarial attacks to fool DNNs when compared to prior methods and enables improved robustness.

Contributions. The key contribution of this paper is the development and evaluation of the DTW-AR framework for studying adversarial robustness of DNNs for time-series domain. Specific list includes:

- Theoretical and empirical analysis to demonstrate the

• The authors are with the School of Electrical Engineering and Computer Science, Washington State University, Pullman, WA, 99164. E-mail: {taha.belkhouja, yan.yan1, jana.doppa}@wsu.edu

effectiveness of DTW over the standard l_2 distance metric for adversarial robustness studies.

- Principled algorithm using DTW measure to efficiently create diverse adversarial examples via random alignment paths justified by theoretical analysis.
- Experimental evaluation of DTW-AR on diverse real-world benchmarks and comparison with state-of-the-art baselines. The code and data are available on a GitHub repository and will be made public.
- The source code of DTW-AR algorithms is available at <https://github.com/tahabelhouja/DTW-AR>

2 BACKGROUND AND PROBLEM SETUP

Let $X \in \mathbb{R}^{n \times T}$ be a multi-variate time-series signal, where n is the number of channels and T is the window-size of the signal. We consider a DNN classifier $F_\theta : \mathbb{R}^{n \times T} \rightarrow \mathcal{Y}$, where θ stands for parameters and \mathcal{Y} is the set of classification labels. Table 1 summarizes the different mathematical notations used in this paper.

TABLE 1
Mathematical notations used in this paper.

Variable	Definition
F_θ	DNN classifier with parameters θ
$\mathbb{R}^{n \times T}$	Time-series input space, where n is the number of channels and T is the window-size
X_{adv}	Adversarial example generated from time-series input $X \in \mathbb{R}^{n \times T}$
\mathcal{Y}	Set of output class labels
$DTW(\cdot, \cdot)$	Dynamic time warping distance
P	Alignment path: a sequence of cost matrix cells $\{(i, j)\}_{i \leq T, j \leq T}$
C	Alignment cost matrix generated by dynamic programming with elements $C_{i,j}$
δ	Distance bound constraint

X_{adv} is called an adversarial example of X if:

$$\{X_{adv} \mid DIST(X_{adv}, X) \leq \delta \text{ and } F_\theta(X) \neq F_\theta(X_{adv})\}$$

where δ defines the neighborhood of highly-similar examples for input X using a distance metric $DIST$ to create worst-possible outcomes from the learning agent’s perspective. Note that adversarial examples depend on the target concept because it defines the notion of invariance we care about.

Challenges for time-series data. The standard l_p -norm distance doesn’t capture the unique characteristics (e.g., fast-pulse oscillations, sharp peaks) and the appropriate notion of invariance for time-series signals. Hence, l_p -norm based perturbations can lead to a time-series signal that semantically belongs to a different class-label. Our experiments show that small perturbations result in adversarial examples whose l_2 distance from the original time-series signal is greater than the distance between time-series signals from two different class labels (see Section 5.2). Therefore, we need to study new methods by exploiting the structure and unique characteristics of time-series signals.

DTW measure. The DTW measure between two uni-variate signals X and $Z \in \mathbb{R}^T$ is computed via a cost matrix $C \in \mathbb{R}^{T \times T}$ using a dynamic programming (DP) algorithm with time-complexity $\mathcal{O}(T^2)$. The cost matrix is computed recursively using the following equation:

$$C_{i,j} = d(X_i, Z_j) + \min \{C_{i-1,j}, C_{i,j-1}, C_{i-1,j-1}\} \quad (1)$$

where $d(\cdot, \cdot)$ is any given distance metric (e.g., $\|\cdot\|_p$ norm). The DTW measure between signals X and Z is $DTW(X, Z) = C_{T,T}$. The sequence of cells $P = \{c_{i,j} = (i, j)\}$ contributing to $C_{T,T}$ is the *optimal alignment path* between X and Z . Figure 1 provides illustration for an optimal alignment path. We note that the diagonal path corresponds to the Euclidean distance metric.

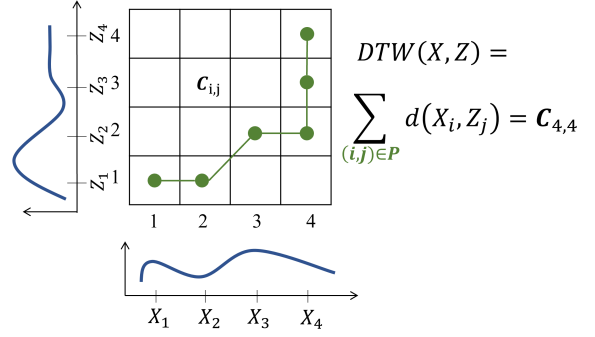


Fig. 1. Illustration of DTW alignment between two uni-variate signals X and Z of length 4. The optimal alignment path (shown in green color) is $P = \{(1, 1), (2, 1), (3, 2), (4, 2), (4, 3), (4, 4)\}$.

For the multi-variate case, where X and $Z \in \mathbb{R}^{n \times T}$, to measure the DTW measure using Equation 1, we have $d(X_i, Z_j)$ with $X_i, Z_j \in \mathbb{R}^n$ [9]. We define the distance function $dist_P(X, Z)$ between time-series inputs X and Z according to an alignment path P using the following equations:

$$dist_P(X, Z) = \sum_{(i,j) \in P} d(X_i, Z_j) \quad (2)$$

Hence, the DTW measure between X and Z is given by:

$$DTW(X, Z) = \min_P dist_P(X, Z) \quad (3)$$

3 DYNAMIC TIME WARPING BASED ADVERSARIAL ROBUSTNESS FRAMEWORK

The DTW-AR framework creates targeted adversarial examples for time-series domain using the DTW measure as illustrated in Figure 2. For any given time-series input X , DNN classifier F_θ , and distance bound δ , we solve an optimization problem to identify an adversarial example X_{adv} which is within DTW measure δ to the original time-series signal X . In what follows, we first provide empirical and theoretical results to demonstrate the suitability of DTW measure over Euclidean distance for adversarial robustness studies in the time-series domain (Section 3.1). Next, we introduce the optimization formulation based on the DTW measure to create adversarial examples and describe its main drawbacks (Section 3.2). Finally, we explain our key insight of using stochastic alignment paths to successfully overcome those drawbacks to efficiently create diverse adversarial examples and provide theoretical justification (Section 3.3).

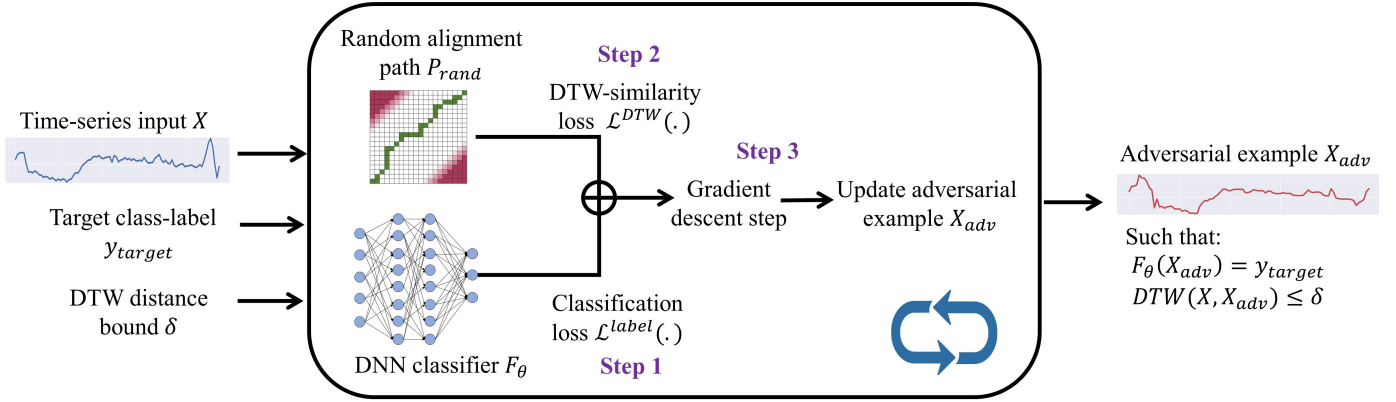


Fig. 2. Overview of the DTW-AR framework to create targeted adversarial examples. Given an input X , a target class-label y_{target} and a distance bound δ , DTW-AR aims to identify an adversarial example X_{adv} using a random alignment path P_{rand} . DTW-AR solves an optimization problem involving a DTW-similarity loss and a classification loss using a random alignment path P_{rand} and a DNN classifier F_θ . Using different random alignment paths, DTW-AR will be able to create diverse adversarial examples which meet the DTW measure bound δ .

3.1 Effectiveness of DTW measure measure

Empirical justification. As we argued before, the standard l_2 distance is impractical for adversarial learning in time-series domain. Perturbations based on Euclidean distance can result in adversarial time-series signals which semantically belong to a different class-label. Figure 3 provides an intuitive illustration of suitability of DTW over l_2 distance and is based on the real-world data representation that is provided in Figure 4. It shows the difference in the true data distribution

between data points in the original space. Figure 4 shows MDS results of SC dataset. We can clearly see how the data from different class labels are better clustered in the DTW space compared to the Euclidean space, as provided in Figure 4. An adversarial example for an SC data point in the green-labeled class is more likely to semantically belong to the red-labeled distribution in the Euclidean space. However, in the DTW space, the adversarial example is more likely to remain in the green-labeled space, while only being misclassified by the DNN classifier due the adversarial problem.

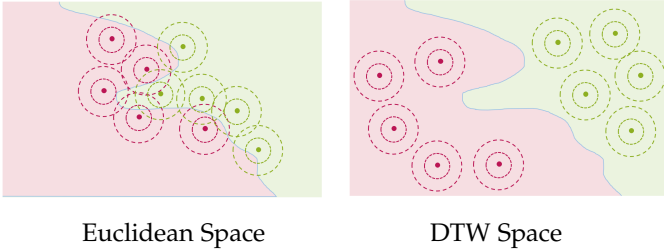


Fig. 3. Illustration of the suitability of DTW over Euclidean distance using the true data distribution from two classes shown in red and green colors. The concentric circles represent the close-similarity area of each input instance (i.e., center) using the corresponding distance measure.

in Euclidean space (i.e., l_2 is used as the similarity measure) and in DTW space (i.e., DTW is used as the similarity measure) for two classes shown in red and green colors. The concentric circles represent the close-similarity area around each input instance (i.e., center) where adversarial examples are considered. We can observe that in the Euclidean space, adversarial example of an input instance can belong to another class label, which is not the case in the DTW space. This simple illustration shows how DTW-AR can generate effective adversarial examples due to the appropriate bias of DTW for time-series domain.

We also show that this abstraction is true for real-world data. We employ multi-dimensional scaling (MDS), a visual representation of dissimilarities between sets of data points [10], to compare DTW and Euclidean spaces. MDS is a dimensionality reduction method that preserves the distances

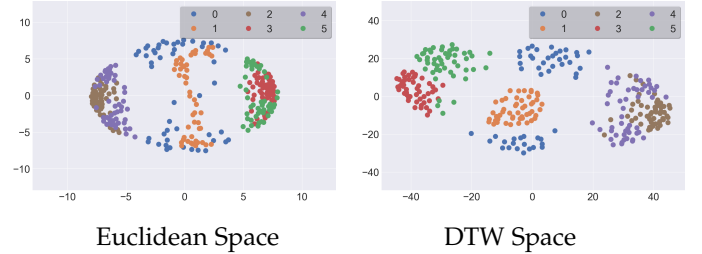


Fig. 4. Multi-dimensional scaling results showing the labeled data distribution in Euclidean space (left column) and DTW space (right column) for the SC dataset. DTW space exhibits better clustering for same-class data than Euclidean space.

Theoretical justification. We prove that the DTW measure allows DTW-AR to explore a larger space of candidate adversarial examples when compared to perturbations based on the Euclidean distance, i.e., identifies blind spots of prior methods. This result is based on the fact that the point-to-point alignment (i.e., Euclidean distance) between two time-series signals is not always the optimal alignment. Hence, the existence of adversarial examples which are similar based on DTW and may not be similar based on the Euclidean distance. To formalize this intuition, we provide Observation 1. We characterize the effectiveness of DTW-AR based attack as better for their ability to extend the space of attacks based on the Euclidean distance and their potential to fool DNN classifiers that rely on Euclidean distance for adversarial training. Our experimental results demonstrate that DTW-AR generates effective adversarial examples to fool the target

DNN classifiers by leveraging the appropriate bias of DTW for time-series data.

Observation 1. Let l_2 be the equivalent of Euclidean distance using the cost matrix in the DTW space. $\forall X \in \mathbb{R}^{n \times T}$ ($n > 1, T > 1$), there exists $\epsilon \in \mathbb{R}^{n \times T}$ and an alignment path P such that $\text{dist}_P(X, X + \epsilon) \leq \delta$ and $l_2(X, X + \epsilon) > \delta$.

Theorem 1. For a given input space $\mathbb{R}^{n \times T}$, a constrained DTW space for adversarial examples is a strict superset of a constrained euclidean space for adversarial examples. If $X \in \mathbb{R}^{n \times T}$:

$$\left\{ X_{adv} \mid \text{DTW}(X, X_{adv}) \leq \delta \right\} \supset \left\{ X_{adv} \mid \|X - X_{adv}\|_2^2 \leq \delta \right\} \quad (4)$$

As an extension of Observation 1, the above theorem states that in the space where adversarial examples are constrained using a DTW measure bound, there exists more adversarial examples that are not part of the space of adversarial examples based on the Euclidean distance for the same bound (i.e., blind spots). This result implies that DTW measure has an appropriate bias for the time-series domain. We present the proofs of both Observation 1 and Theorem 1 in the **Appendix**. Hence, our DTW-AR framework is *potentially* capable of creating more effective adversarial examples than prior methods based on l_2 distance for the same distance bound constraint. These adversarial examples are potentially more effective as they are able to break deep models by leveraging the appropriate bias of DTW measure.

However, to convert this potential to reality, we need an algorithm that can efficiently search this larger space of attacks to identify most or all adversarial examples which meet the DTW measure bound. Indeed, developing such an algorithm is one of the key contributions of this paper.

3.2 Naive optimization based formulation and challenges to create adversarial examples

To create adversarial examples to fool the given DNN F_θ , we need to find an optimized perturbation of the input time-series X to get X_{adv} . Our approach is based on minimizing a *loss function* \mathcal{L} using gradient descent that achieves two goals. 1) Misclassification goal: Adversarial example X_{adv} to be mis-classified by F_θ as a target class-label y_{target} ; and 2) DTW similarity goal: close DTW-based similarity between time-series X and adversarial example X_{adv} .

To achieve the mis-classification goal, we employ the formulation of [11] to define a loss function:

$$\mathcal{L}^{label}(X_{adv}) = \max \left[\max_{y \neq y_{target}} (\mathcal{S}_y(X_{adv})) - \mathcal{S}_{y_{target}}(X_{adv}), \rho \right] \quad (5)$$

where $\rho < 0$. It ensures that the adversarial example will be classified by the DNN as class-label y_{target} with a confidence $|\rho|$ using the output of the pre-softmax layer $\{\mathcal{S}_y\}_{y \in Y}$.

To achieve the DTW similarity goal, we need to create X_{adv} for a given time-series input X such that $\text{DTW}(X, X_{adv}) \leq \delta$. We start by a naive optimization over the DTW measure using the Soft-DTW measure $\text{SDTW}(X, X_{adv})$ [12]. Hence, the DTW similarity loss function is:

$$\mathcal{L}^{DTW}(X_{adv}) = \text{SDTW}(X, X_{adv}) \quad (6)$$

The final loss function \mathcal{L} we want to minimize to create optimized adversarial example X_{adv} is:

$$\mathcal{L}(X_{adv}) = \mathcal{L}^{label}(X_{adv}) + \mathcal{L}^{DTW}(X_{adv}) \quad (\star)$$

We operate under white-box setting and can employ gradient descent to minimize the loss function in Equation \star over X_{adv} . This approach works for black-box setting also. In this work, we consider the general case where we do not query the black-box target DNN classifier. We show through experiments that the created adversarial examples can generalize to fool other black-box DNNs.

Challenges of Naive approach. Recall that our overall goal is to identify most or all targeted adversarial time-series examples that meet the DTW measure bound. This will allow us to improve the robustness of DNN model using adversarial training. This naive approach has two main drawbacks.

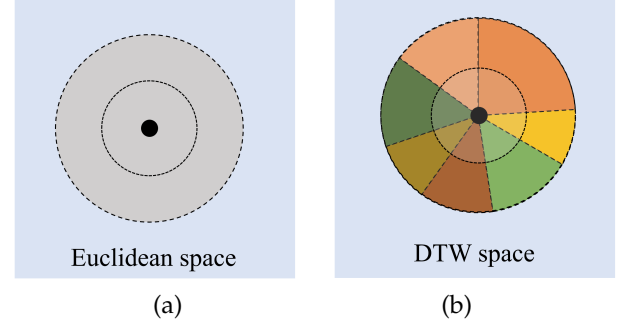


Fig. 5. Illustration of the close-similarity space around a given time-series signal (black center) in the Euclidean and DTW space. Using l_2 norm is sufficient to explore the entire Euclidean space around the input. However, in the DTW space, each colored section corresponds to one adversarial example that meets the DTW measure bound constraint. Each of them can be found using only a subset of candidate alignment paths.

- *Single adversarial example.* The method allows us to only find one valid adversarial example out of multiple solution candidates from the search space because it operates on a single optimal alignment path. Using a single alignment path (whether the diagonal path for Euclidean distance or the optimal alignment path generated by DTW), the algorithm will be limited to the adversarial examples which use that single alignment. In Figure 5, we provide a conceptual illustration of $S_{ADV}(X)$, the set of all adversarial examples X_{adv} which meet the distance bound constraint $\text{DTW}(X, X_{adv}) \leq \delta$. In the Euclidean space, using l_2 norm is sufficient to explore the entire search space around the original input to create adversarial examples. However, in the DTW space, each colored section in $S_{ADV}(X)$ can only be found using a subset of candidate alignment paths.

- *High computational cost.* DTW is non-differentiable and approximation methods are often used in practice. These methods require $\mathcal{O}(n \cdot T^2)$ to fill the cost matrix and $\mathcal{O}(T)$ to backtrack the optimal alignment path. These steps are computationally-expensive. Gradient-based optimization iteratively updates the adversarial example X_{adv} to achieve the DTW similarity goal, i.e., $\text{DTW}(X, X_{adv}) \leq \delta$, and the mis-classification goal, i.e., $F_\theta(X_{adv}) = y_{target}$. Standard algorithms such as projected gradient descent (PGD) [13] and Carloni & Wagner (CW) [11] require a large number

of iterations to generate valid adversarial examples. This is also true for the recent computer vision specific adversarial algorithms [14], [15]. For time-series signals arising in many real-world applications, the required number of iterations to create successful attacks can grow even larger. We need to compute DTW measure in each iteration as the optimal DTW alignment path changes over iterations. Therefore, it is impractical to use the exact DTW computation algorithm to create adversarial examples. We also show that the existing optimized approaches to estimate the DTW measure remain computationally expensive for an adversarial framework. We provide results to quantify the runtime cost in our experimental evaluation.

Algorithm 1 DTW-AR based Adversarial Algorithm

Input: time-series X ; DNN classifier F_θ ; target class-label y_{target} ; learning rate η ; maximum iterations MAX

Output: adversarial example X_{adv}

- 1: $P_{rand} \leftarrow$ random alignment path
 - 2: Initialization: $X_{adv} \leftarrow X$
 - 3: **for** $i=1$ to MAX **do**
 - 4: $\mathcal{L}(X_{adv}) \leftarrow \mathcal{L}^{label}(X_{adv}) + \mathcal{L}^{DTW}(X_{adv}, P_{rand})$
 - 5: Compute gradient $\nabla_{X_{adv}} \mathcal{L}(X_{adv})$
 - 6: Perform gradient descent step:
 $X_{adv} \leftarrow X_{adv} - \eta \times \nabla_{X_{adv}} \mathcal{L}(X_{adv})$
 - 7: **end for**
 - 8: **return** optimized adversarial example X_{adv}
-

3.3 Stochastic alignment paths for the DTW similarity goal and theoretical justification

In this section, we describe the key insight of DTW-AR to overcome the above-mentioned two challenges and provide theoretical justification.

To overcome the above-mentioned two challenges of the naive approach, we propose the use of a random alignment path to create adversarial attacks on DNNs for time-series domain. The key idea is to select a random alignment path P and to execute our adversarial algorithm while constraining over $dist_P(X, X_{adv})$ instead of $DTW(X, X_{adv})$. This choice is justified from a theoretical point-of-view due to the special structure in the problem to create DTW based adversarial examples. Using the distance function $dist_P(X, X_{adv})$, we redefine Equation 6 as follows:

$$\mathcal{L}^{DTW}(X_{adv}, P) = \alpha_1 \times dist_P(X, X_{adv}) - \alpha_2 \times dist_{P_{diag}}(X, X_{adv}) \quad (7)$$

where $\alpha_1 > 0$, $\alpha_2 \geq 0$, P_{diag} is the diagonal alignment path equivalent to the Euclidean distance, and P is a given alignment path ($P \neq P_{diag}$). The first term of Equation 7 is defined to bound the DTW similarity of adversarial example X_{adv} to a threshold δ as stated in Observation 2. The second term represents a penalty term to account for adversarial example with close Euclidean distance to the original input X and pushes the algorithm to look beyond adversarial examples in the Euclidean space. The coefficients α_1 and α_2 contribute in defining the position of the adversarial output in the DTW and/or Euclidean space. If $\alpha_2 \rightarrow 0$, the adversarial example X_{adv} will be highly similarity to the

original input X in the DTW space with no consideration to the Euclidean space. Hence, the adversarial example may be potentially adversarial in the Euclidean space also. However, if $\alpha_2 > 0$, the adversarial output will be highly similar to the original input in the DTW space but out of the scope of adversarial attacks in the Euclidean space (i.e., a blind spot). Recall from Theorem 1 that DTW space allows more candidate adversarial examples than Euclidean space. Hence, this setting allows us to find blind spots of Euclidean space based attacks.

The DTW-AR approach to create adversarial examples is shown in Algorithm 1. We note that the naive approach that uses Soft-DTW with the Carlini & Wagner loss function is a sub-case of DTW-AR as shown below:

$$\begin{aligned} \text{SDTW}(X, X_{adv}) &= \mathcal{L}^{DTW}(X_{adv}, P_{DTW}) = \\ &1 \times dist_{P_{DTW}}(X, X_{adv}) - 0 \times dist_{P_{diag}}(X, X_{adv}) \end{aligned} \quad (8)$$

where P_{DTW} is the optimal DTW alignment path.

Observation 2. Given any alignment path P and two multivariate time-series signals $X, Z \in \mathbb{R}^{n \times T}$. If we have $dist_P(X, Z) \leq \delta$, then $DTW(X, Z) \leq \delta$.

Observation 2 states that $dist_P(X, Z)$ defined with respect to a path P is always an upper bound for $DTW(X, Z)$, since DTW uses the optimal alignment path. Hence, when the alignment path is fixed, the time-complexity is reduced to a simpler similarity measure that requires only $\mathcal{O}(n.T)$, which results in significant computational savings due to repeated calls within the adversarial algorithm.

Our stochastic alignment method also improves the search strategy for finding multiple desired adversarial examples. Suppose $S_{ADV}(X)$ is the set of all adversarial examples X_{adv} which meet the distance bound constraint $DTW(X, X_{adv}) \leq \delta$. Each adversarial example in $S_{ADV}(X)$ can be found using only a subset of candidate alignment paths. By using a stochastic alignment path, we can leverage the large pool of different alignment paths to uncover more than one adversarial example from $S_{ADV}(X)$. On the other hand, if the exact DTW computation based algorithm was feasible, we would only find a *single* X_{adv} , as DTW based algorithm operates on a single optimal alignment path.

Theoretical tightness of bound. While Observation 2 provides an upper bound for the DTW measure, it does not provide any information about the tightness of the bound. To analyze this gap, we need to first define a similarity measure between two alignment paths to quantify their closeness. We define PathSim as a similarity measure between two alignment paths P_1 and P_2 in the DTW cost matrix of time-series signals $X, Z \in \mathbb{R}^{n \times T}$. Let $P_1 = \{c_1^1, \dots, c_k^1\}$ and $P_2 = \{c_1^2, \dots, c_l^2\}$ represent the sequence of cells for paths P_1 and P_2 respectively.

$$\begin{aligned} \text{PathSim}(P_1, P_2) &= \\ &\frac{1}{2T} \left(\sum_{c_i^1} \min_{c_j^2} \|c_i^1 - c_j^2\|_1 + \sum_{c_i^2} \min_{c_j^1} \|c_i^2 - c_j^1\|_1 \right) \end{aligned} \quad (9)$$

As $\text{PathSim}(P_1, P_2)$ approaches 0, P_1 and P_2 are very similar, and they will be the exact same path if $\text{PathSim}(P_1, P_2) = 0$. For $X, Z \in \mathbb{R}^{n \times T}$, two very similar

alignment paths corresponds to a similar feature alignment between X and Z . Theorem 2 shows the tightness of the bound given in Observation 2 using the path similarity measure defined above.

Theorem 2. For a given input $X \in \mathbb{R}^{n \times T}$ and a random alignment path P_{rand} , the resulting adversarial example X_{adv} from the minimization over $dist_{P_{rand}}(X, X_{adv})$ is equivalent to minimizing over $DTW(X, X_{adv})$. For any X_{adv} generated by DTW-AR using P_{rand} , we have:

$$\begin{cases} PathSim(P_{rand}, P_{DTW}) = 0 \\ \& \\ dist_{P_{rand}}(X, X_{adv}) = DTW(X, X_{adv}) \end{cases} \quad (10)$$

where P_{DTW} is the optimal alignment path found using DTW computation between X and X_{adv} .

Similarity measure PathSim definition. For DTW-AR, we rely on a stochastic alignment path to compute $dist_P$ defined in Equation 2. To improve our understanding of the behavior of DTW-AR framework based on stochastic alignment paths, we propose to define a similarity measure that we call PathSim. This measure quantifies the similarities between two alignment paths P_1 and P_2 in the DTW cost matrix for two time-series signals $X, Z \in \mathbb{R}^{n \times T}$. If we denote the alignment path sequence $P_1 = \{c_1^1, \dots, c_k^1\}$ and $P_2 = \{c_1^2, \dots, c_l^2\}$, then we can measure their similarity as defined in Equation 9.

This definition is a *valid* similarity measure as it satisfies all the distance axioms [16]:

Non-negativity: By definition, $PathSim(P_1, P_2)$ is a sum of l_1 distances, which are all positives. Hence, $PathSim(P_1, P_2) \geq 0$.

Unicity: $PathSim(P_1, P_2) = 0$

$$\begin{aligned} &\iff \frac{1}{2T} \left(\sum_{c_i^1} \min_{c_j^2} \|c_i^1 - c_j^2\|_1 + \sum_{c_i^2} \min_{c_j^1} \|c_i^2 - c_j^1\|_1 \right) = 0 \\ &\iff \sum_{c_i^1} \min_{c_j^2} \|c_i^1 - c_j^2\|_1 + \sum_{c_i^2} \min_{c_j^1} \|c_i^2 - c_j^1\|_1 = 0 \end{aligned}$$

As we have a sum equal to 0 of all positive terms, we can conclude that each term $(\min \|\cdot\|_1)$ is equal to 0: $PathSim(P_1, P_2) = 0$

$$\begin{aligned} &\iff \forall i : \|c_i^1 - c_i^2\|_1 = 0 \\ &\iff \forall i : c_i^1 = c_i^2 \end{aligned}$$

As both paths have the same sequence of cells, we can safely conclude that $PathSim(P_1, P_2) = 0 \iff P_1 = P_2$:

Symmetric Property:

$$\begin{aligned} PathSim(P_1, P_2) &= \frac{1}{2T} \left(\sum_{c_i^1} \min_{c_j^2} \|c_i^1 - c_j^2\|_1 + \sum_{c_i^2} \min_{c_j^1} \|c_i^2 - c_j^1\|_1 \right) \\ &= \frac{1}{2T} \left(\sum_{c_i^2} \min_{c_j^1} \|c_i^2 - c_j^1\|_1 + \sum_{c_i^1} \min_{c_j^2} \|c_i^1 - c_j^2\|_1 \right) \\ &= PathSim(P_2, P_1) \end{aligned}$$

Note that the triangle inequality is not applicable as the alignment path spaces does not support additive operations.

This similarity measure quantifies the similarity between two alignment paths as it measures the l_1 distance between the different cells of each path. The multiplication factor $1/2T$ is introduced to prevent scaling of the measure for large T values for a given time-series input space $\mathbb{R}^{n \times T}$.

In Figure 6, we visually show the relation between PathSim measure and the alignment path for a given cost matrix. We observe that when $PathSim(P_1, P_2) \rightarrow 0$, P_1 and P_2 are very similar, and they will be the exact same path if $PathSim(P_1, P_2) = 0$. For $PathSim(P_1, P_2) \gg 0$, the alignment path will go through different cells which are far-placed from each other in the cost matrix.

Empirical tightness of bound. Figure 7 shows that over the iterations of the DTW-AR algorithm, the updated adversarial example yields to an optimal alignment path that is more similar to the input random path. This result strongly demonstrate that Theorem 2 holds empirically.

Corollary 1. Let P_1 and P_2 be two alignment paths such that $PathSim(P_1, P_2) > 0$. If X_{adv}^1 and X_{adv}^2 are the adversarial examples generated using DTW-AR from any given time-series X using paths P_1 and P_2 respectively such that $DTW(X, X_{adv}^1) = \delta$ and $DTW(X, X_{adv}^2) = \delta$, then X_{adv}^1 and X_{adv}^2 are not necessarily the same.

Theorem 2 shows that the adversarial example generation using DTW-AR is equivalent to the ideal setting where it is possible to optimize $DTW(X, X_{adv})$. The above corollary extends Theorem 2 to show that if we employ different alignment paths within Algorithm 1, we will be able to find more adversarial examples which meet the distance bound in contrast to the naive approach.

4 RELATED WORK

Adversarial methods. Prior work on adversarial examples mostly focus on image and text domains [4], [5]. Such methods include Carlini & Wagner attack [11], boundary attack [17], and universal attacks [18]. Recent work focuses on regularizing adversarial example generation methods to obey intrinsic properties of images [19], [20], [21]. In NLP domain, methods to fool text classifiers employ the saliency map of input words to generate adversarial examples while preserving meaning to a human reader in white-box setting [22]. DeepWordBug [23] employs a black-box strategy to fool classifiers with simple character-level transformations. Since characteristics of time-series (e.g., fast-pace oscillations, sharp peaks) are different from images and text, prior methods are not suitable to capture the appropriate notion of invariance for time-series domain.

Adversarial robustness. Adversarial training is one of the strongest empirical defense methods against adversarial attacks [13], [24]. This involves employing attack methods to create adversarial examples to augment the training data for improving robustness. Stability training [25] is an alternative method that explicitly optimizes for robustness by defining a loss function that evaluates the classifier on small perturbations of clean examples. This method yield to a deep network that is stable against natural and adversarial

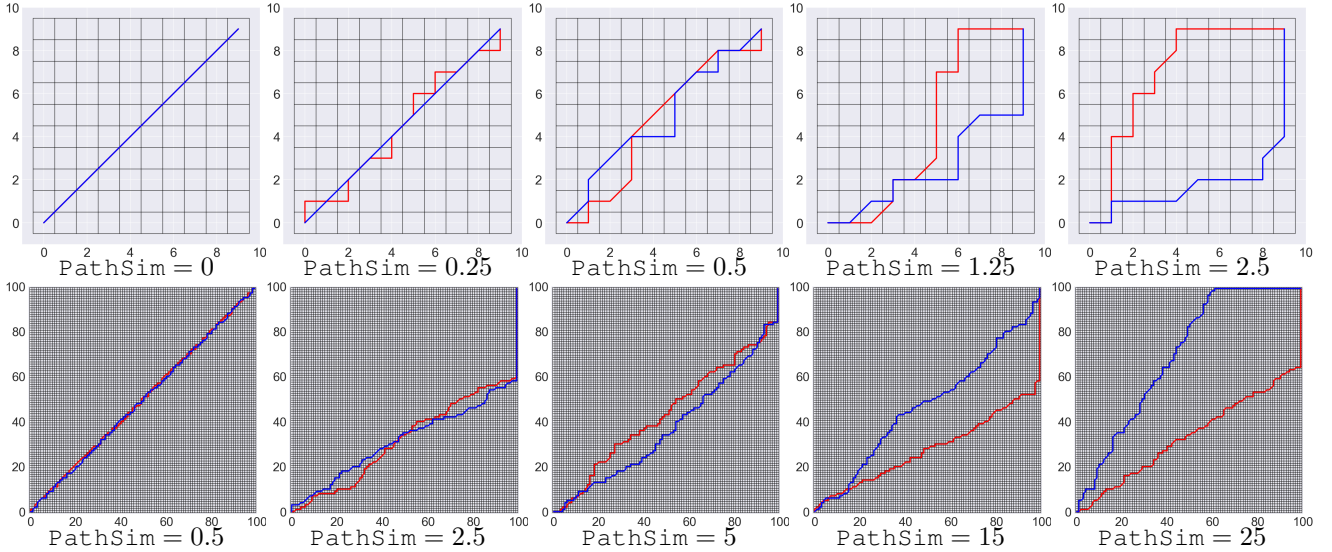


Fig. 6. Visualization of PathSim values along different example alignment paths in $\mathbb{R}^{n \times 10}$ (First row) and $\mathbb{R}^{n \times 100}$ (Second row) spaces.

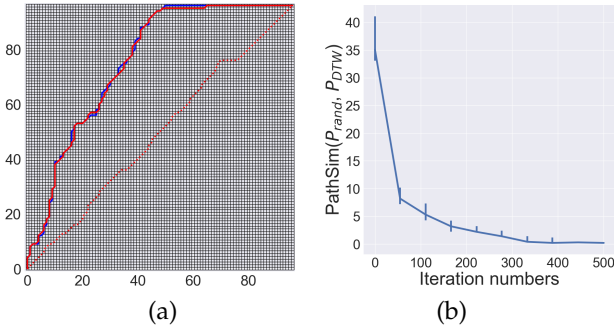


Fig. 7. (a) Example of the convergence of the optimal alignment path between the adversarial example and the original example at the start of the algorithm (dotted red path) and at the end (red path) to the given random alignment path (blue path). (b) PathSim score of the optimal alignment path between the adversarial example and the original example and the given random path for the ECG200 dataset averaged over multiple random alignment paths.

distortions in the visual input. There are other defense methods which try to overcome injection of adversarial examples [26], [27], [28]. However, for time-series domain, as l_p -norm based perturbations may not guarantee preserving the semantics of true class label, adversarial examples may mislead DNNs during adversarial training resulting in accuracy degradation.

Adversarial attacks for time-series domain. There is little to no principled prior work on adversarial methods for time-series. Fawaz et al., [29] employed the standard Fast Gradient Sign method [30] to create adversarial noise with the goal of reducing the confidence of deep convolutional models for classifying *uni-variate* time-series. Network distillation is employed to train a student model for creating adversarial attacks [31]. However, this method is severely limited: it can generate adversarial examples for only a small number of target labels and cannot guarantee generation of adversarial example for every input. [32] tried to address adversarial examples with elastic similarity measures, but does not propose any elastic-measure based attack algorithm.

Time-series pre-processing methods. A possible solution to overcome the Euclidean distance concerns is to introduce pre-processing steps that are likely to improve the existing frameworks. Simple pre-processing steps such as MinMax-normalization or z-normalization only solves problems such as scaling problem. However, they do not address any concern about signal-warping or time-shifts. Other approaches rely on learning feature-preserving representations. A well-known example is the GRAIL [33] framework. This framework aims to learn compact time-series representations that preserve the properties of a pre-defined comparison function such as DTW. The main concern about feature-preserving pre-processing steps is that the representation learnt is not reversible. In other words, a real-world time-series signal cannot be generated from the estimated representation. The goal of adversarial attacks is to create real-world time-series that can be used to fool any DNN. Such challenges would limit the usability and the generality of methods based on pre-processing steps to study the robustness of DNNs for time-series data.

In summary, existing methods for time-series domain are lacking in the following ways: 1) they do not create targeted adversarial attacks; and 2) they employ l_p -norm based perturbations which do not take into account the unique characteristics of time-series data.

5 EXPERIMENTS AND RESULTS

We empirically evaluate the DTW-AR framework and discuss the results along different dimensions.

5.1 Experimental setup

Datasets. We employ the UCR datasets benchmark [34]. We present the results on five representative datasets (AtrialFibrillation, Epilepsy, ERing, Heartbeat, RacketSports) from diverse domains noting that our findings are general as shown by the results on remaining UCR datasets in the **Appendix**. We employ the standard training/validation/testing splits from these benchmarks.

Configuration of algorithms. We employ a 1D-CNN architecture for the target DNNs. We operate under a white-box (WB) setting for creating adversarial examples to fool *WB* model. To assess the effectiveness of attacks, we evaluate the attacks under the black-box (BB) setting and to fool *BB* model. Neural architectures of both *WB* and *BB* models are in the Appendix. The adversarial algorithm has no prior knowledge/querying ability of target DNN classifiers. Target DNNs include: 1) DNN model with a different architecture trained on clean data (*BB*); 2) DNNs trained using augmented data from baselines attacks that are not specific to image domain: Fast Gradient Sign method (*FGS*) [30], Carlini & Wagner (*CW*) attack [11], and Projected Gradient Descent (*PGD*) [13]; and 3) DNN models trained using stability training [25] (*STN*) for learning robust classifiers.

Evaluation metrics. We evaluate attacks using the efficiency metric $\alpha_{Eff} \in [0, 1]$ over the created adversarial examples. α_{Eff} (higher means better attacks) measures the capability of adversarial examples to fool a given DNN F_θ to output the target class-label. α_{Eff} is calculated as the fraction of adversarial examples that are predicted correctly by the classifier: $\alpha_{Eff} = \frac{\# \text{ Adv. examples s.t. } F(X) = y_{target}}{\# \text{ Adv. examples}}$. We evaluate adversarial training by measuring the accuracy of the model to predict ground-truth labels of adversarial examples. A DNN classifier is robust if it is successful in predicting the true label of any given adversarial example.

5.2 Results and Discussion

Spatial data distribution with DTW. We have shown in Figure 4 how the data from different class labels are better clustered in the DTW space compared to the Euclidean space. These results demonstrate that DTW suits better the time-series domain as generated adversarial examples lack true-label guarantees. Moreover, Euclidean distance based attacks can potentially create adversarial examples that are *inconsistent* for adversarial training. Our analysis showed that for datasets such as *WISDM*, there are time-series signals from different classes with l_2 -distances ≤ 2 , while *PGD* or *FGS* require $\epsilon \geq 2$ to create successful adversarial examples for more than 70% time-series instances. We provide in the Appendix an additional visualization of the adversarial examples using DTW.

Admissible alignment paths. The main property of DTW alignment is the one-to-many match between time-steps to identify similar warped pattern. Intuitively, if an alignment path matches few time-steps from the first signal with too many steps in the second signal, both signals are not considered similar. Consequently, the optimal path would be close to the corners of the cost matrix. Figure 8 provides a comparison between two adversarial signals generated using a green colored path closer to the diagonal vs. a red colored path that is close to the corners. We can see that the red path produces an adversarial example that is not similar to the original input. Hence, we limit the range of the random path P_{rand} used to a safe range omitting the cells at the top and bottom halves of the top-left and bottom-right corners.

Multiple diverse adversarial examples using DTW-AR. In section 3.2, we argued that using stochastic alignment paths, we can create multiple diverse adversarial time-series

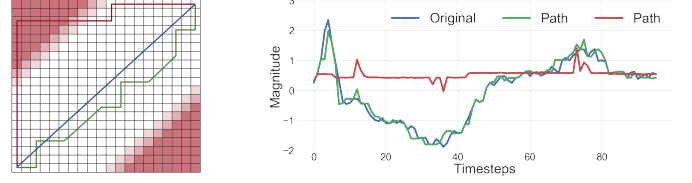


Fig. 8. Effect of alignment path on adversarial example.

TABLE 2

Average percentage of dissimilar adversarial examples created by DTW-AR using stochastic alignment paths for a given time-series. The threshold ϵ_{sim} determines whether two adversarial examples are dissimilar or not based on l_2 and DTW measures.

	$\epsilon_{sim} \ l_2 \text{ norm}$			$\epsilon_{sim} \text{ DTW}$		
	0.01	0.05	0.1	0.01	0.05	0.1
Atrial Fibrillation	98%	90%	87%	100%	100%	98%
Epilepsy	99%	96%	93%	100%	100%	97%
ERing	99%	95%	93%	100%	100%	98%
Heartbeat	99%	94%	92%	100%	99%	98%
RacketSports	99%	94%	92%	100%	100%	96%

examples within the same DTW measure bound. DTW-AR method leverages the large pool of candidate alignment paths to uncover more than one adversarial example as illustrated in Figure 5. To further test this hypothesis, we perform the following experiment. We sample a subset of different (using *PathSim*) alignment paths $\{P_{rand}\}_i$ and execute DTW-AR algorithm to create adversarial examples for the same time-series X . Let $X_{adv,i}$ be the adversarial example generated from X using $P_{rand,i}$. We measure the similarities between the generated $\{X_{adv}\}_i$ using DTW and l_2 distance. If the distance between two adversarial examples is less than a threshold ϵ_{sim} , then they are considered the same adversarial example. Table 2 shows the percentage of adversarial examples generated using different alignment paths from a given time-series signal that are not similar to any other adversarial example. We conclude that DTW-AR algorithm indeed creates multiple different adversarial examples from a single time-series signal for the same DTW measure bound.

Empirical justification for Theorem 2. We provided a proof for the gap between creating an adversarial example using the proposed DTW-AR algorithm and an ideal DTW algorithm. In Figure 7(a), we provide an illustration of the optimal alignment path update using DTW-AR. This experiment was performed on the ECG200 dataset as an example (noting that we observed similar patterns for other datasets as well): the blue path represents the selected random path to be used by DTW-AR and the red path represents the optimal alignment path computed by DTW. At the beginning, the optimal alignment path (dotted path) and the random path are dissimilar. However, as the execution of DTW-AR progresses, the updated adversarial example yields to an optimal alignment path similar to the random path. In Figure 7(b), we show the progress of the *PathSim* score as a function of the iteration numbers of Algorithm 1. This figure shows the convergence of the *PathSim* score to 0. These

strong results confirm the main claim of Theorem 2 that the resulting adversarial example X_{adv} from the minimization over $dist_{P_{rand}}(X, X_{adv})$ is equivalent to minimizing over $DTW(X, X_{adv})$!

Loss function scaling. As the final loss function is using two different terms to create adversarial attacks, the absence of a scaling parameter can affect the optimization process. In Figure 10, we demonstrate that empirically, the first term of the Equation \star plateaus at ρ before minimizing \mathcal{L}^{DTW} . The figure shows the progress of both \mathcal{L}^{label} and $\mathcal{L}^{DTW} = \alpha_1 \times dist_P(X, X_{adv})$ over the first 100 iterations of DTW-AR algorithm. We conclude that there is no need to scale the loss function noting that our findings were similar for other time-series datasets. In the general case, if a given application requires attention to scaling both terms (\mathcal{L}^{DTW} and \mathcal{L}^{label}), the learning rate can be adjusted to two different values: Instead of having $\eta * \nabla L = \eta * \nabla L^{label} + \eta * \nabla L^{DTW}$, we can use a learning rate pair $\eta = (\eta_1, \eta_2)$ and gradient descent step becomes $\eta * \nabla L = \eta_1 * \nabla L^{label} + \eta_2 * \nabla L^{DTW}$.

Effectiveness of adversarial attacks. Results of the fooling rate of DTW-AR generated attacks for different models are shown in Figure 9. We observe that under the white-box setting (WB model), we have $\alpha_{Eff}=1$. This shows that for any y_{target} , DTW-AR successfully generates an adversarial example for every input in the dataset. For black-box setting (BB model) and other models using baseline attacks for adversarial training, we see that DTW-AR attack is highly effective for most cases. We conclude that these results support the theoretical claim made in Theorem 1 by showing that standard l_2 -norm based attacks have blind spots and the DTW bias is appropriate for time-series. The importance of α_2 in Equation 7 is shown to improve the fooling rate of adversarial examples. To implement DTW-AR adversarial attacks, we have fixed $\alpha_1 = 0.5$ and $\alpha_2 = 0.5$ for Equation 7. The importance of α_2 is to push the algorithm to create adversarial examples out of the scope of the Euclidean space as shown in Figure 11. The adversarial examples with $\alpha_2 \neq 0$ evade DNNs with adversarial training baselines better than the examples with $\alpha_2 = 0$.

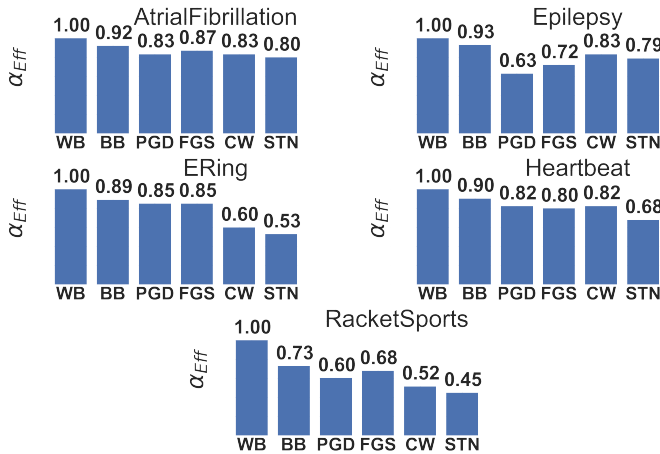


Fig. 9. Results for the effectiveness of adversarial examples from DTW-AR on different DNNs under white-box (WB) and black-box (BB) settings, and using adversarial training baselines (PGD, FGS, CW and STN) on different datasets.

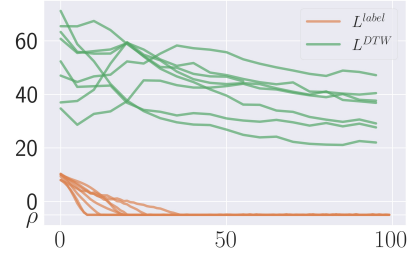


Fig. 10. The progress of loss function values over the first 100 iterations of DTW-AR on different examples from ATRIALFIBRILLATION datasets. We observe that empirically, the Equation \star plateaus at ρ before minimizing \mathcal{L}^{DTW} .

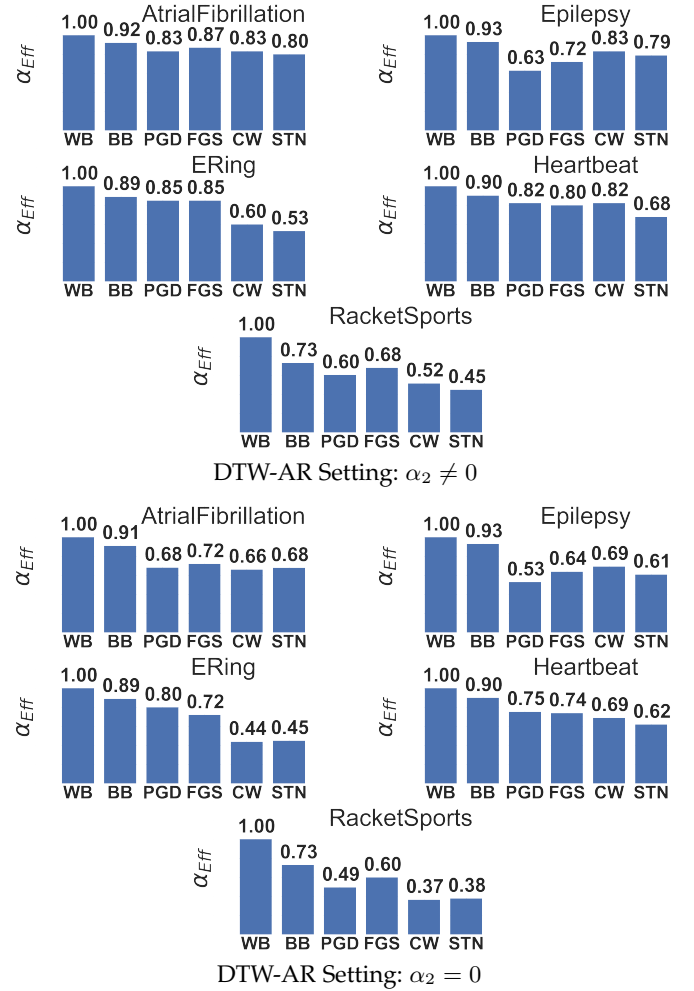


Fig. 11. Results for the effectiveness of adversarial examples from DTW-AR on different DNNs under white-box (WB) and black-box (BB) settings, and using adversarial training baselines (PGD, FGS, CW and STN) on different datasets under two attack settings: $\alpha_2 \neq 0$ and $\alpha_2 = 0$.

DTW-AR based adversarial training. Our hypothesis is that l_2 -based perturbations lack true-label guarantees and can degrade the overall performance of DNNs. Figure 12 shows the accuracy of different DNNs after adversarial training on clean data. This performance is relative to the clean testing set of each dataset. We observe that all l_2 -based methods degrade the performance using adversarial training for at least one dataset. However, for many datasets,

the performance is visibly improved using DTW-AR based adversarial training. Compared to standard training (i.e., no augmented adversarial examples), the performance on *AtrialFibrillation* improved using DTW-AR while it declined with other methods; and on *HeartBeat*, DTW-AR based training improves from 70% to 75%. To evaluate the

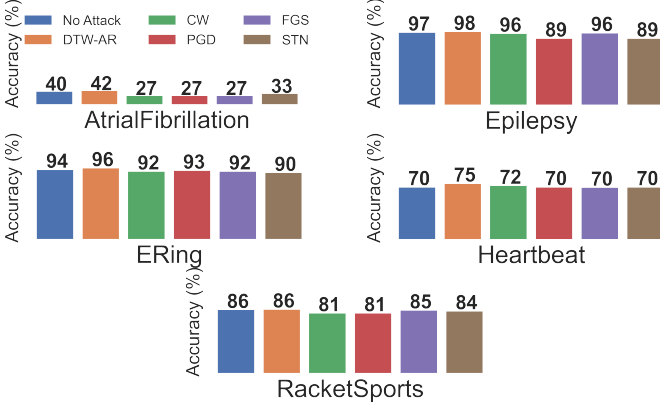


Fig. 12. Results of adversarial training using baseline attacks and DTW-AR, and comparison with standard training without adversarial examples (No Attack) to classify clean data.

accuracy of DTW-AR in predicting the ground-truth label of adversarial examples, we create adversarial examples using a given attack algorithm and label each example with the true class-label of the corresponding clean time-series input. Figure 13 shows the results of DTW-AR based adversarial training using *WB* architecture. In this experiment, we con-

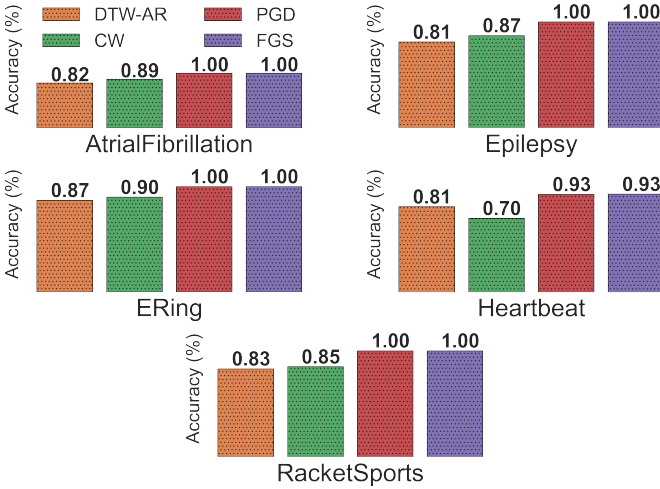


Fig. 13. Results of DTW-AR based adversarial training to predict the true labels of adversarial examples generated by DTW-AR and the baseline attack methods. The adversarial examples considered are those which successfully fooled DNNs that do not use adversarial training.

sider the adversarial examples that have successfully fooled the original DNN (i.e., no adversarial training). We observe that DNNs using DTW-AR for adversarial training are able to predict the original label of adversarial examples with high accuracy. We can see how FGS and PGD attacks cannot evade the DTW-AR based trained deep model for almost any dataset. These results show that DTW-AR significantly improves the robustness of deep models for time-series data

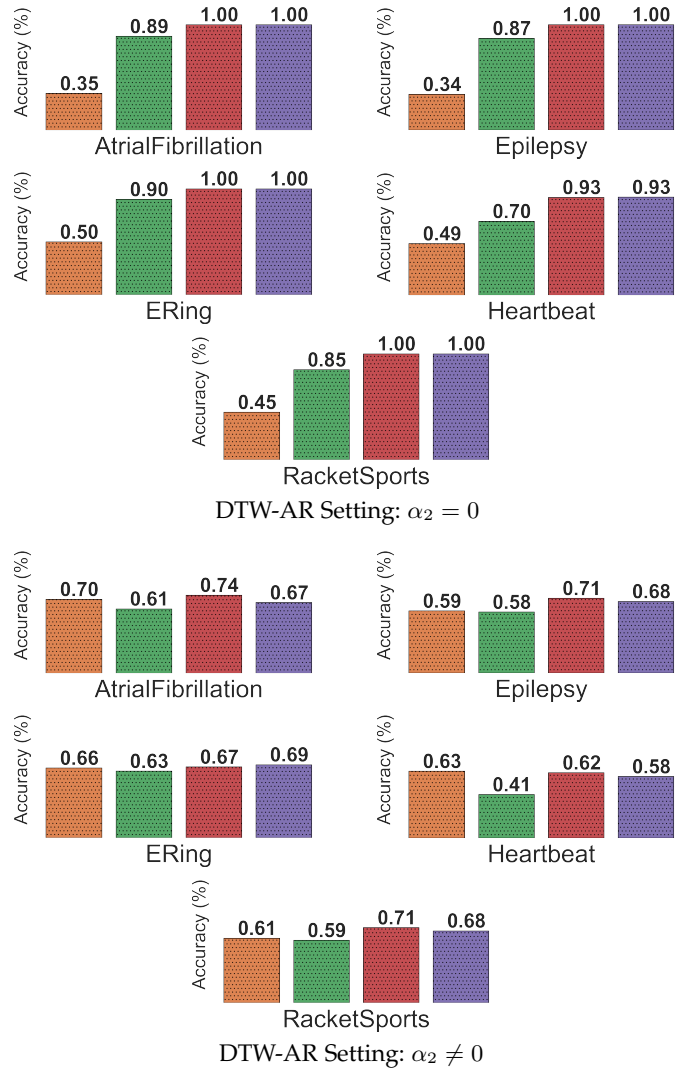
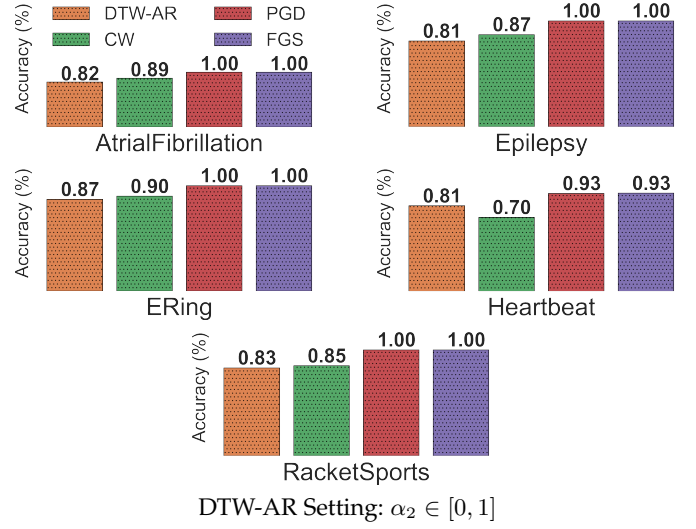


Fig. 14. Results of DTW-AR based adversarial training to predict the true labels of adversarial examples generated by DTW-AR and the baseline attack methods. The adversarial examples considered are those that successfully fooled DNNs that do not use adversarial training.

to evade attacks generated by DTW-AR and other baseline

attacks. For the adversarial training, we employ several values to create adversarial examples to be used in the training phase. We have set $\alpha_1 \in [0.1, 1]$ and $\alpha_2 \in [0, 1]$. In Figure 14, we show the role of the term α_2 of Equation 7 in the robustness of the DNN. $\alpha_2 \in [0, 1]$ ensures diverse DTW-AR examples to increase the robustness of a given DNN. When set to 0, we see that there is no significant difference in the performance against baseline attacks. However, the DNN cannot defend against all DTW-AR attacks. We can also observe that the setting where α_2 is strictly different than 0 is the worst, as the DNN does not learn from the adversarial examples that are found in the Euclidean space by DTW-AR or the given baselines.

Naive approach: Carlini & Wagner with Soft-DTW. Recall that naive approach uses DTW measure within the Carlini & Wagner loss function. SoftDTW [12] allows us to create a differentiable version of DTW measure. Hence, we provide results for this naive approach to verify if the use of Soft-DTW with existing Euclidean distance based methods can solve the challenges for the time-series domain mentioned in this paper. We compare the DTW-AR algorithm with the CW-SDTW that plugs Soft-DTW within the Carlini & Wagner algorithm instead of the standard l_2 distance. CW-SDTW has the following limitations when compared against DTW-AR:

- The time-complexity of Soft-DTW is quadratic in the dimensionality of time-series input space, whereas the distance computation in DTW-AR is linear.
- The CW-SDTW attack method is a sub-case of the DTW-AR algorithm. If DTW-AR algorithm uses the optimal alignment path instead of a random path, the result will be equivalent to a CW-SDTW attack.
- For a given time-series signal, CW-SDTW will output one single adversarial example and cannot uncover multiple adversarial examples which meet the DTW measure bound. However, DTW-AR algorithm gives the user control over the alignment path and can create multiple diverse adversarial examples.

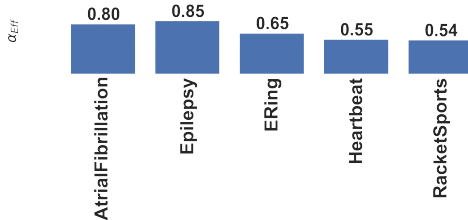


Fig. 15. Results for the effectiveness of adversarial examples from DTW-AR against adversarial training using examples created by CW-SDTW on different datasets.

In conclusion, both challenges that were explained in the *Challenges of Naive approach* in Section 3.1 cannot be solved using CW-SDTW. As a consequence, the robustness goal aimed by this paper cannot be achieved using solely CW-SDTW. Indeed, our experiments support this hypothesis. Figure 15 shows that DTW-AR is successful to fool a DNN that uses adversarial examples from CW-SDTW for adversarial training. This shows that our proposed framework is better than this naive baseline. Figure 16 shows that DTW-AR significantly improves the robustness of deep models for

time-series as it is able to evade attacks generated by CW-SDTW. Both these experiments demonstrate that CW-SDTW is neither able to create stronger attacks nor a more robust deep model when compared to DTW-AR.

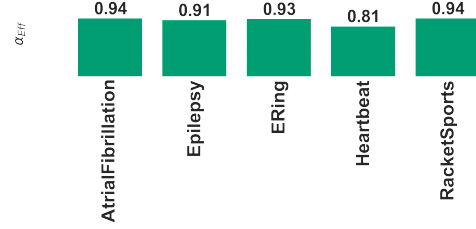


Fig. 16. Results for the effectiveness of adversarial training using DTW-AR based examples against adversarial attacks from CW-SDTW on different datasets.

Comparison with Karim et al., [31]. The approach from Karim et al., [31] employs network distillation to train a student model for creating adversarial attacks. However, this method is severely limited: only a small number of target classes yield adversarial examples and the method does not guarantee the generation of an adversarial example for every input. Karim et al., have shown that for many datasets, this method creates a limited number of adversarial examples in the white-box setting. To test the effectiveness of this attack against DTW-AR, Figure 29 shows the success rate of deep model from DTW-AR based adversarial training to predict the true labels of the attacks generated by the method from Karim et al., on different datasets.

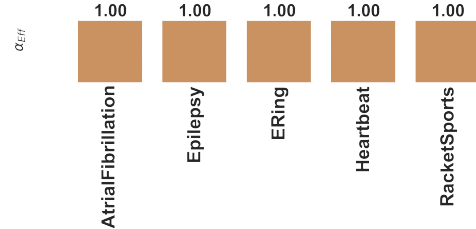


Fig. 17. Results of the success rate of deep model from DTW-AR based adversarial training to predict the true label of adversarial attacks generated using method in [31].

DTW-AR outperforms [31] due to following reasons:

- DTW-AR generates at least one adversarial example for every input $X \in \mathbb{R}^{n \times T}$ as shown in our experiments.
- Adversarial examples created by DTW-AR are highly effective against deep models relying on [31] for adversarial training as this baseline fails to create adversarial examples for many inputs and target classes (shown in [31]).
- Adversarial examples created by the method from [31] does not evade deep models from DTW-AR based adversarial training.

Computational runtime of DTW-AR vs. DTW. As explained in the technical section, optimization based attack algorithm requires a large number of iterations to create a highly-similar adversarial example. For example, 10^3

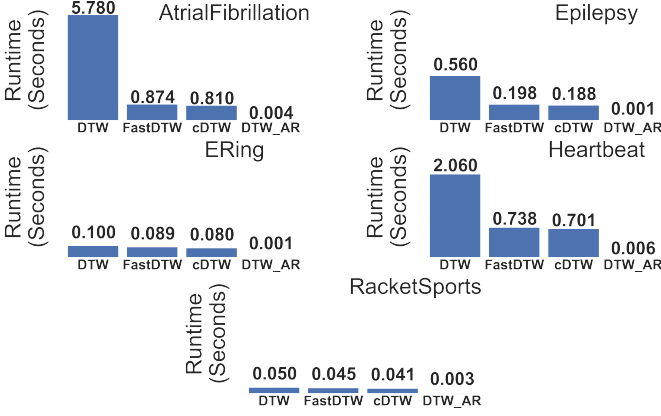


Fig. 18. Average runtime **per iteration** for standard DTW, FastDTW, cDTW, and DTW-AR (on NVIDIA Titan Xp GPU).

iterations is the required default choice for CW to create successful attacks, especially, for large time-series in our experiments. The exact DTW method is non-differentiable, thus, it is not possible to perform experiments to compare DTW-AR method to the exact DTW method. Hence, we assume that each iteration will compute the optimal DTW path and use it instead of the random path. To assess the runtime of computing the DTW measure, we employ three different approaches: 1) The standard DTW algorithm, 2) FastDTW [35] that is introduced as a very fast and accurate DTW variant that works on lower resolutions of the data, and 3) cDTW [36] that is a different variant of FastDTW. We provide the runtime of performing each iteration using the different algorithms in Figure 18. We can clearly observe that DTW-AR is orders of magnitude faster than the standard DTW and the accelerated DTW algorithms. The overall computational cost will be significantly reduced using DTW-AR compared to exact DTW or soft-DTW [12] for large-size time-series signals.

DTW-AR extension to other multivariate DTW measures. The DTW-AR framework relies on the distance function $dist_P(X, Z) = \sum_{(i,j) \in P} d(X_i, Z_j)$ between two time-series signals X and Z according to an alignment path P to measure their similarity. Extending the DTW notion from univariate to multivariate is a known problem, where depending on the application, researchers' suggest to change the definition of $dist_P(X, Z)$ to better fit the characteristics of the application at hand. In all cases, DTW-AR relies on using the final cost matrix $DTW(X, Z) = \min_P dist_P(X, Z)$ using dynamic programming $C_{i,j} = d(X_i, Z_j) + \min \{C_{i-1,j}, C_{i,j-1}, C_{i-1,j-1}\}$. Therefore, the use of different variants of $dist_P(X, Z)$ (e.g., DTW_I or DTW_D [9]) will only affect the cost matrix values, but will not change the assumptions and applicability of DTW-AR. Therefore, DTW-AR is general and can work with any variant of DTW. In Figure 19, we demonstrate that using a different family of DTW (DTW_I) does not have a major impact on DTW-AR's performance and effectiveness. The performance of DTW-AR framework using both alternative measures of multi-variate DTW does not affect the overall performance. Therefore, for a given specific application, the practitioner can configure DTW-AR appropriately.

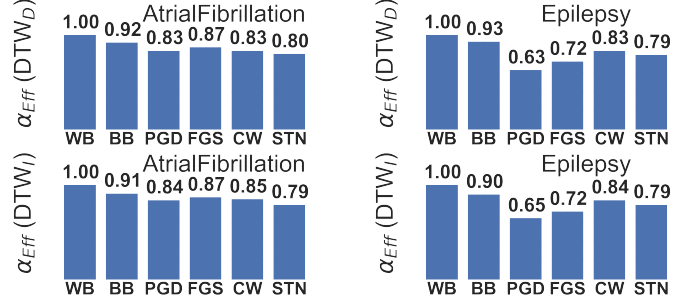


Fig. 19. Results for the effectiveness of adversarial examples from DTW-AR using DTWAdaptive [9] (DTW_D top row, DTW_I bottom row) on different DNNs under different settings.

5.3 Summary of Experimental Results

Our experimental results supported all the claims made in Section 3. The summary list includes:

- Figure 4 showed that DTW space is more suitable for adversarial studies in the time-series domain than Euclidean distance to support Theorem 1.
- Using stochastic alignment paths, DTW-AR creates multiple diverse adversarial examples to support Corollary 1 (Table 2), which is impossible using the optimal alignment path.
- Figure 7 provides empirical justification for Theorem 2 showing that minimizing over a given alignment path is equivalent to minimizing using exact DTW method (bound is tight).
- Figure 9 shows that adversarial examples created by DTW-AR have higher potential to break time-series DNN classifiers.
- Figures 12 and 13 show that DTW-AR based adversarial training is able to improve the robustness of DNNs against baseline adversarial attacks.
- Figure 15 and 16 shows that DTW-AR outperforms the naive approach CW-SDTW that uses SoftDTW with the Carlini & Wagner loss function. We also demonstrated several limitations of CW-SDTW to achieve the robustness goal aimed by this paper.
- Figure 18 clearly demonstrates that DTW-AR significantly reduces the computational cost compared to existing approaches of computing the DTW measure for creating adversarial examples.
- Figure 19 demonstrates that DTW-AR can generalize to any multivariate DTW measure (such as DTWAdaptive [9]) without impacting on its performance and effectiveness.

6 CONCLUSIONS

We introduced the DTW-AR framework to study adversarial robustness of deep models for the time-series domain using dynamic time warping measure. This framework creates effective adversarial examples by overcoming the limitations of prior methods based on Euclidean distance. We theoretically and empirically demonstrate the effectiveness of DTW-AR to fool deep models for time-series data and to improve their robustness. We conclude that the time-series domain needs focused investigation for studying robustness of deep models by shedding light on the unique challenges.

REFERENCES

- [1] A. Ignatov, "Real-time human activity recognition from accelerometer data using convolutional neural networks," *Applied Soft Computing*, vol. 62, pp. 915–922, 2018.
- [2] A. M. Özbayoglu, M. U. Gudelek, and O. B. Sezer, "Deep learning for financial applications : A survey," *Appl. Soft Comput.*, vol. 93, p. 106384, 2020.
- [3] Z. Zheng, Y. Yang, X. Niu, H.-N. Dai, and Y. Zhou, "Wide and deep convolutional neural networks for electricity-theft detection to secure smart grids," *IEEE Transactions on Industrial Informatics*, 2017.
- [4] Z. Kolter and A. Madry, "Tutorial adversarial robustness: Theory and practice," *NeurIPS*, 2018.
- [5] W. Y. Wang, S. Singh, and J. Li, "Deep adversarial learning for NLP," in *Proceedings of the 2019 Conference of the North American Chapter of the Association for Computational Linguistics: Human Language Technologies, NAACL-HLT 2019, Minneapolis, MN, USA, June 2, 2019, Tutorial Abstracts*, A. Sarkar and M. Strube, Eds. Association for Computational Linguistics, 2019, pp. 1–5.
- [6] H. Sakoe, "Dynamic-programming approach to continuous speech recognition," in *1971 Proc. the International Congress of Acoustics, Budapest*, 1971.
- [7] M. Müller, "Dynamic time warping," *Information retrieval for music and motion*, pp. 69–84, 2007.
- [8] D. J. Berndt and J. Clifford, "Using dynamic time warping to find patterns in time series," in *KDD workshop*, vol. 10, no. 16. Seattle, WA, USA, 1994, pp. 359–370.
- [9] M. Shokoohi-Yekta, B. Hu, H. Jin, J. Wang, and E. Keogh, "Generalizing dtw to the multi-dimensional case requires an adaptive approach," *Data mining and knowledge discovery*, vol. 31, no. 1, pp. 1–31, 2017.
- [10] A. Buja, D. F. Swayne, M. L. Littman, N. Dean, H. Hofmann, and L. Chen, "Data visualization with multidimensional scaling," *Journal of computational and graphical statistics*, vol. 17, no. 2, pp. 444–472, 2008.
- [11] N. Carlini and D. A. Wagner, "Towards evaluating the robustness of neural networks," in *2017 IEEE Symposium on Security and Privacy, SP 2017, San Jose, CA, USA, May 22–26, 2017*. IEEE Computer Society, 2017, pp. 39–57.
- [12] M. Cuturi and M. Blondel, "Soft-dtw: a differentiable loss function for time-series," in *International Conference on Machine Learning*. PMLR, 2017, pp. 894–903.
- [13] A. Madry, A. Makelov, L. Schmidt, D. Tsipras, and A. Vladu, "Towards deep learning models resistant to adversarial attacks," in *6th International Conference on Learning Representations, ICLR 2018, Vancouver, BC, Canada, April 30 - May 3, 2018, Conference Track Proceedings*. OpenReview.net, 2018.
- [14] C. Laidlaw and S. Feizi, "Functional adversarial attacks," in *Advances in Neural Information Processing Systems (NeurIPS)*, 2019.
- [15] A. Shafahi, M. Najibi, Z. Xu, J. Dickerson, L. S. Davis, and T. Goldstein, "Universal adversarial training," *Proceedings of the AAAI Conference on Artificial Intelligence*, vol. 34, 2020.
- [16] M. J. Cullinane, "Metric axioms and distance," *The Mathematical Gazette*, vol. 95, no. 534, pp. 414–419, 2011.
- [17] W. Brendel, J. Rauber, and M. Bethge, "Decision-based adversarial attacks: Reliable attacks against black-box machine learning models," in *6th International Conference on Learning Representations, ICLR 2018, Vancouver, BC, Canada, April 30 - May 3, 2018, Conference Track Proceedings*. OpenReview.net, 2018.
- [18] S. Moosavi-Dezfooli, A. Fawzi, O. Fawzi, and P. Frossard, "Universal adversarial perturbations," in *2017 IEEE Conference on Computer Vision and Pattern Recognition, CVPR 2017, Honolulu, HI, USA, July 21–26, 2017*. IEEE Computer Society, 2017, pp. 86–94.
- [19] C. Laidlaw and S. Feizi, "Functional adversarial attacks," in *Advances in Neural Information Processing Systems (NeurIPS)*, 2019, pp. 10408–10418.
- [20] C. Xiao, J. Zhu, B. Li, W. He, M. Liu, and D. Song, "Spatially transformed adversarial examples," in *6th International Conference on Learning Representations, ICLR 2018, Vancouver, BC, Canada, April 30 - May 3, 2018, Conference Track Proceedings*. OpenReview.net, 2018.
- [21] H. Hosseini, B. Xiao, M. Jaiswal, and R. Poovendran, "On the limitation of convolutional neural networks in recognizing negative images," in *16th International Conference on Machine Learning and Applications (ICMLA)*. IEEE, 2017.
- [22] S. Samanta and S. Mehta, "Towards crafting text adversarial samples," *arXiv preprint arXiv:1707.02812*, 2017.
- [23] J. Gao, J. Lanchantin, M. L. Soffa, and Y. Qi, "Black-box generation of adversarial text sequences to evade deep learning classifiers," in *IEEE Security and Privacy Workshops (SPW)*, 2018, pp. 50–56.
- [24] F. Tramer, N. Carlini, W. Brendel, and A. Madry, "On adaptive attacks to adversarial example defenses," *arXiv preprint arXiv:2002.08347*, 2020.
- [25] S. Zheng, Y. Song, T. Leung, and I. J. Goodfellow, "Improving the robustness of deep neural networks via stability training," in *2016 IEEE Conference on Computer Vision and Pattern Recognition, CVPR 2016, Las Vegas, NV, USA, June 27–30, 2016*. IEEE Computer Society, 2016, pp. 4480–4488.
- [26] A. Athalye, N. Carlini, and D. Wagner, "Obfuscated gradients give a false sense of security: Circumventing defenses to adversarial examples," ser. *Proceedings of Machine Learning Research*, J. Dy and A. Krause, Eds., vol. 80. Stockholmsmässan, Stockholm Sweden: PMLR, 10–15 Jul 2018, pp. 274–283.
- [27] N. Papernot, P. McDaniel, X. Wu, S. Jha, and A. Swami, "Distillation as a defense to adversarial perturbations against deep neural networks," in *IEEE Symposium on Security and Privacy (SP)*, 2016, pp. 582–597.
- [28] F. Tramèr, A. Kurakin, N. Papernot, I. J. Goodfellow, D. Boneh, and P. D. McDaniel, "Ensemble adversarial training: Attacks and defenses," in *6th International Conference on Learning Representations, ICLR 2018, Vancouver, BC, Canada, April 30 - May 3, 2018, Conference Track Proceedings*. OpenReview.net, 2018.
- [29] H. I. Fawaz, G. Forestier, J. Weber, L. Idoumghar, and P. Muller, "Adversarial attacks on deep neural networks for time series classification," in *International Joint Conference on Neural Networks, IJCNN 2019 Budapest, Hungary, July 14–19, 2019*. IEEE, 2019, pp. 1–8.
- [30] A. Kurakin, I. J. Goodfellow, and S. Bengio, "Adversarial examples in the physical world," in *5th International Conference on Learning Representations, ICLR 2017, Toulon, France, April 24–26, 2017, Workshop Track Proceedings*. OpenReview.net, 2017.
- [31] F. Karim, S. Majumdar, and H. Darabi, "Adversarial attacks on time series," *IEEE Transactions on pattern analysis and machine intelligence*, 2020.
- [32] I. Oregi, J. D. Ser, A. Pérez, and J. A. Lozano, "Adversarial sample crafting for time series classification with elastic similarity measures," in *Intelligent Distributed Computing XII, 12th International Symposium on Intelligent Distributed Computing, IDC 2018, Bilbao, Spain, 15–17 October 2018*, ser. *Studies in Computational Intelligence*, vol. 798. Springer, 2018, pp. 26–39.
- [33] J. Paparrizos and M. J. Franklin, "Grail: Efficient time-series representation learning," *Proc. VLDB Endowment*, 2019.
- [34] A. Bagnall, J. Lines, W. Vickers, and E. Keogh, "The UEA & UCR time series classification rep." www.timeseriesclassification.com, 2020.
- [35] S. Salvador and P. Chan, "Toward accurate dynamic time warping in linear time and space," *Intelligent Data Analysis*, 2007.
- [36] R. Wu and E. J. Keogh, "Fastdtw is approximate and generally slower than the algorithm it approximates," 2020. [Online]. Available: <https://arxiv.org/abs/2003.11246>
- [37] M. Abadi et al., "TensorFlow: Large-scale machine learning on heterogeneous systems," 2015, software available from tensorflow.org. [Online]. Available: <https://www.tensorflow.org/>
- [38] N. Papernot, P. McDaniel, I. Goodfellow, S. Jha, Z. B. Celik, and A. Swami, "Practical black-box attacks against machine learning," in *Proceedings of Asia Conference on Computer and Communications Security (ASIACCS)*. ACM, 2017.
- [39] N. Papernot et al., "Technical report on the cleverhans v2.1.0 adversarial examples library," *arXiv preprint arXiv:1610.00768*, 2018.

APPENDIX A

EXPERIMENTAL AND IMPLEMENTATION DETAILS

Datasets. We have employed the standard benchmark training, validation, and testing split on the datasets. All datasets are publicly available from the UCR repository [34]. We employ the datasets in the main paper on which the classifier is able to have a performance better than random guessing. Experiments on the effectiveness of adversarial attack that aim to fool poor classifiers would not exhibit trust-worthy results, as the classifier originally is unable to predict clean data.

DNN architectures. To evaluate the DTW-AR framework, we employ two different 1D-CNN architectures — A_0 and A_1 — to create two DNNs: WB uses A_0 to evaluate the adversarial attack under a white-box setting, and is trained using clean training examples. BB uses the architecture A_1 to evaluate the black-box setting for a model trained using clean examples. The architecture details of the deep learning models are presented in Table 3.

TABLE 3
Details of DNN architectures. C: Convolutional layers, K: kernel size, P: max-pooling kernel size, and R: rectified linear layer.

	C	K	C	K	P	R	R
A_0	x	x	66	12	12	1024	x
A_1	100	5	50	5	4	200	100

DTW-AR implementation. We implemented the DTW-AR framework using TensorFlow 2 [37]. The parameter ρ that was introduced in Equation 5 plays an important role in the algorithm.

$$\mathcal{L}^{label}(X_{adv}) = \max_{y \neq y_{target}} [\max_y (\mathcal{S}_y(X_{adv})) - \mathcal{S}_{y_{target}}(X_{adv}), \rho] \quad (5)$$

ρ will push gradient descent to minimize mainly the second term (\mathcal{L}^{DTW}) when the first term plateaus at ρ . Otherwise, the gradient can minimize the general loss function by pushing \mathcal{L}^{label} to $-\infty$, which is counter-productive for our goal. In all our experiments, we employ $\rho = -5$ for \mathcal{L}^{label} in Equation 5 for a good confidence in the classification score. A good confidence score is important for the attack’s effectiveness in a black-box setting. Black-box setting assumes that information about the target deep model including its parameters θ are not accessible. In general, the attacker will create a proxy deep model to mimic the behavior of the target model using regular queries. This technique can be more effective when a target scenario is well-defined [24], [38]. However, in this work, we consider the general case where we do not query the black-box target DNN classifier for a better assessment of the proposed framework. Figure 20 shows the role of ρ value in enhancing DTW-AR attacks in a black-box setting on ECG200 dataset noting that we see similar patterns for other datasets as well. Adversarial examples are generated using a maximum of 5×10^3 iterations of gradient descent with the fixed learning rate $\eta=0.01$. After all the iterations, the final adversarial

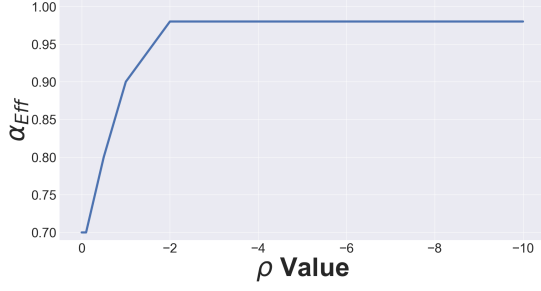


Fig. 20. Results for the fooling rate on ECG200 dataset w.r.t different ρ values for a black-box attack setting.

output is chosen from the iteration with the lowest DTW loss provided from Equation 7.

$$\mathcal{L}^{DTW}(X_{adv}, P) = \alpha_1 \times \text{dist}_P(X, X_{adv}) - \alpha_2 \times \text{dist}_{P_{diag}}(X, X_{adv}) \quad (7)$$

Experimentally, we notice that for $d(\cdot, \cdot)$ in Equation 1 of the main paper, there is no influence on the performance between choosing $p = 1, 2$ or ∞ for $d(\cdot, \cdot) = \|\cdot\|_p$. However, for datasets in $\mathbb{R}^{n \times T}$ with $n \geq 2$, we do not use $p = \infty$ as the dimensions are not normalized and data points will be compared only along the dimension with the greater magnitude.

Implementation of baselines. The baseline methods for CW, PGD, and FGS were implemented using the CleverHans library [39] with updates to TensorFlow 2. For FGS and PGD algorithms, we employed a minimal perturbation factors ($\epsilon < 1$) for two main reasons. First, larger perturbations significantly degrade the overall performance of the adversarial training and potentially creates adversarial signals that are semantically different than the original time-series input. Second, we want to avoid the risk of leaking label information [13]. STN was implemented using the code provided with the paper [25].

APPENDIX B ADDITIONAL EXPERIMENTAL RESULTS

Results on the full UCR multivariate dataset. First, we provide in Figures 21, 22 and 23 the experiments conducted in the main paper on the **Effectiveness of adversarial attacks** and the **DTW-AR based adversarial training** on all the UCR multivariate dataset to our DTW-AR framework is general and highly-effective for all datasets.

In Figure 21, we can observe that DTW-AR performs lower ($\alpha_{eff} \leq 0.5$) for some cases. We explain below how the other baseline attacks fail to outperform the proposed DTW-AR method on the same datasets. In Figure 24 and 25, we show results to evaluate the effectiveness of baseline attacks against the models shown in Figure 21. These results show that DTW-AR is more effective in fooling DNNs created using baseline attacks-based adversarial training. For datasets where DTW-AR did not succeed in fooling the deep models with a high score, Figure 24 and 25 show that baselines fail to outperform our proposed DTW-AR attack. We also demonstrate in Figure 23 that the baselines are

not suitable for time-series domain since DTW-AR based adversarial training is able to defend against these attacks.

Results and Discussion on l_1 and l_∞ . Figure 26 shows the MDS results of SC and Plane in the space using l_1 as a similarity measure (left) and in the space using l_∞ as a similarity measure (right). We can observe that similar to the Euclidean space, there is a substantial entanglement between different classes. Thus, using l_1 and l_∞ comes with similar drawbacks to using the Euclidean space for adversarial studies.

Figure 27 and 28 show the results of DTW-AR based adversarial training against adversarial attacks generated using l_1 and l_∞ as a metric.

We conclude that DTW-AR is able to generalize against attacks in other spaces than the Euclidean one. Since the Manhattan distance is similar to the Euclidean distance in the point-to-point matching, and ∞ -norm describes a signal by solely its maximum value, DTW measure is still considered a better similarity measure. The empirical success of the DTW-AR suggests that the framework can be further analyzed theoretically and empirically for future research into adversarially robust classification when compared to different alternative similarity measures.

Comparison with [31] on the full MV UCR dataset. Figure 29 shows that the observations made within the main paper are still valid over the different datasets.

DTW-AR transferability to RNNs. Prior work has shown that RNN models are competitive with 1D-CNNs for time-series data. Therefore, we evaluate the transferability of adversarial examples from *WB* (1D-CNN) to an RNN model. Figure 30 shows the success rate of DTW-AR adversarial attacks to fool a Long short-term memory (LSTM) model. We can observe that DTW-AR attacks have the transfer potential to fool other non-CNN-based models. Since this paper only studies the setting of no queries to the target deep model, the attacks would have an increased efficiency if the target deep model is available for label queries [38].

Runtime comparison of DTW-AR vs. Carlini & Wagner. As explained in Section 3, one main advantage of DTW-AR is reducing the time complexity of using DTW to create adversarial examples. We provide in Figure 31 a comparison of the average runtime per iteration to create one targeted adversarial example by iterative baseline methods. We note that we only compare to CW because FGSM and PGD are not considered targeted attacks, and Karim et al. [31], fails to create adversarial examples for every input. While we observe that CW is faster, we note that we have already demonstrated empirically (Figure 21 and 24) that DTW-AR always outperforms CW in both effectiveness of adversarial examples and adversarial training. We also observe differences in the DTW-AR’s runtime across datasets. DTW-AR is relatively quick for small-size data such as *RacketSports* (30×6) and slower for large-size data such as *HeartBeat* (405×61). The additional runtime cost is explained by the proposed loss function in Equation 7 that guarantees a highly-similar adversarial example. For future work, we aim to optimize the implementation of DTW-AR to further reduce the runtime on large time-series datasets.

Results on the UCR univariate datasets. To show the effec-

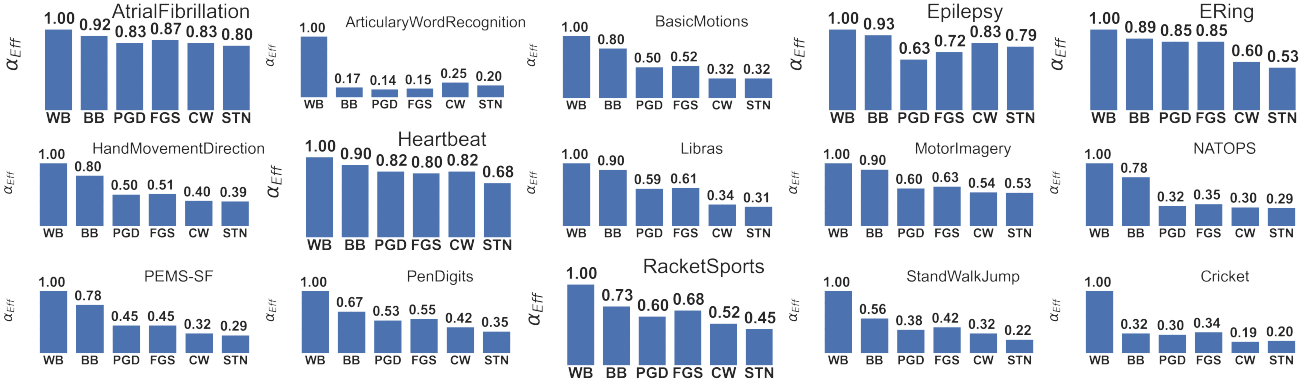


Fig. 21. Results for the effectiveness of adversarial examples from DTW-AR on different DNNs under white-box (WB) and black-box (BB) settings, and using adversarial training baselines (PGD, FGS, CW and STN) on all the UCR multivariate datasets

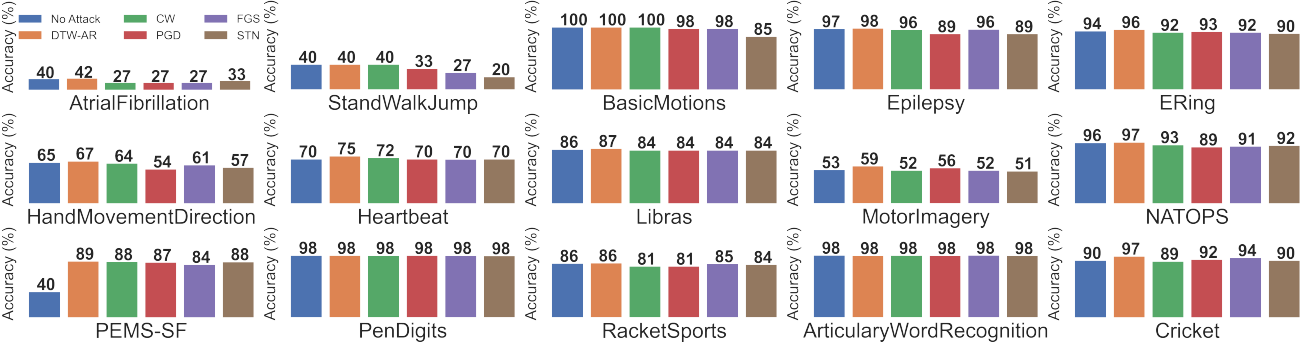


Fig. 22. Results of adversarial training using baseline attacks and DTW-AR on all the UCR multivariate datasets, and comparison with standard training without adversarial examples (No Attack) to classify clean data.

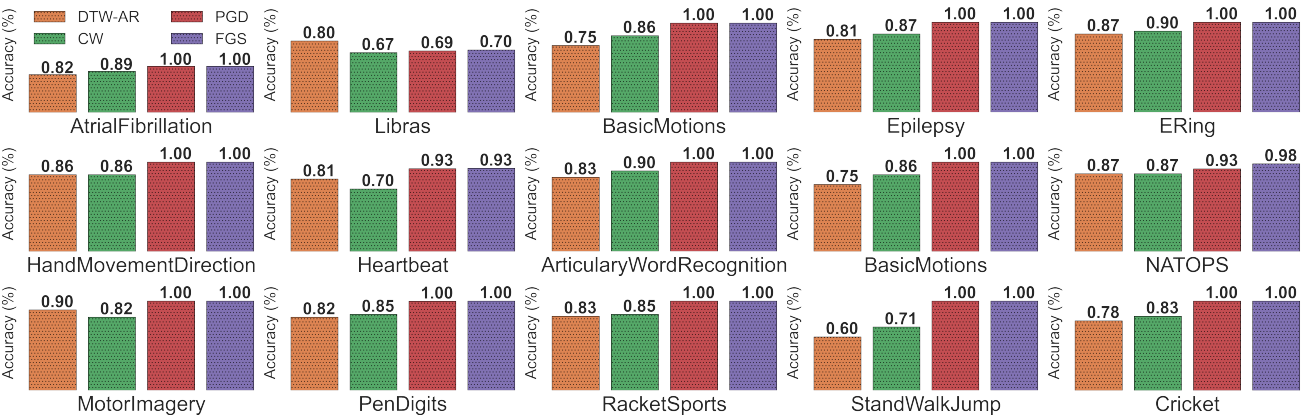


Fig. 23. Results of DTW-AR based adversarial training to predict the true labels of adversarial examples generated by DTW-AR and the baseline attack methods on all the UCR multivariate datasets. The adversarial examples considered are those that successfully fooled DNNs that do not use adversarial training.

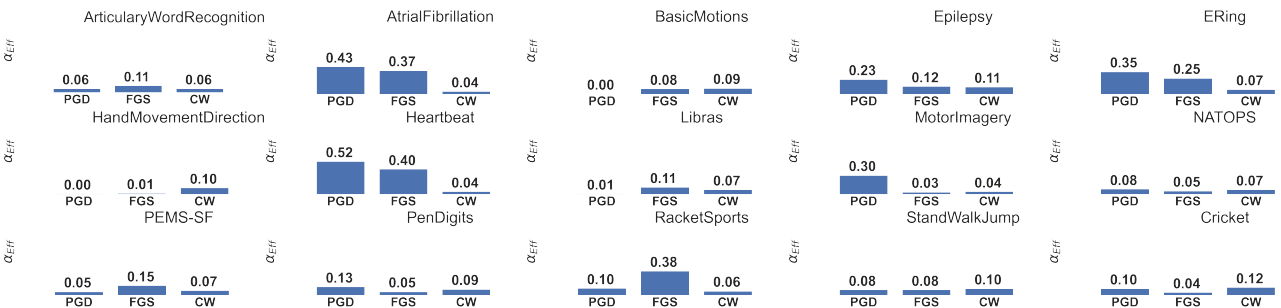


Fig. 24. Results for the effectiveness of adversarial examples from CW on different deep models using adversarial training baselines (PGD, FGS, CW).

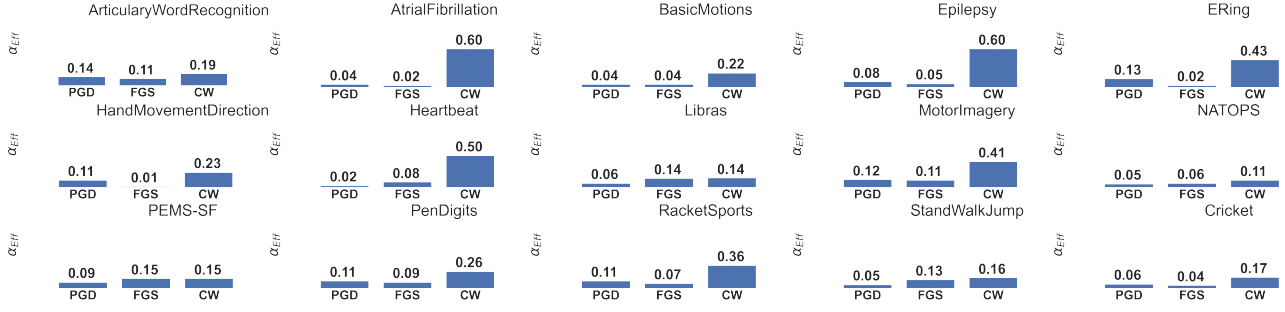


Fig. 25. Results for the effectiveness of adversarial examples from PGD and FGS on different deep models using adversarial training baselines (PGD, FGS, CW).

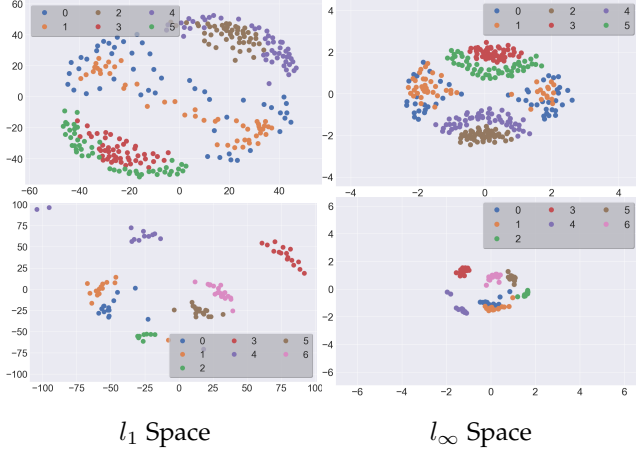


Fig. 26. Multi-dimensional scaling results showing the labeled data distribution in spaces using l_1 as a similarity measure (left column) and l_∞ (right column) for two datasets: SC (top row) and Plane (bottom row).

tiveness of our proposed method, we additionally evaluate DTW-AR on univariate datasets from the UCR time-series benchmarks repository [34]. We show the results of DTW-AR based adversarial training to predict the ground-truth labels of adversarial attacks generated by DTW-AR and the baseline attack methods on the univariate datasets in Figure 32. We observe similar results as the datasets shown in the main paper. DTW-AR is successful in identifying attacks from the baseline methods by creating robust deep models. These strong results show that DTW-AR outperforms baselines for creating more effective adversarial attacks and yields to more robust DNN classifiers. We conclude that the proposed DTW-AR framework is generic, and more suitable for time-series domain to create robust deep models.

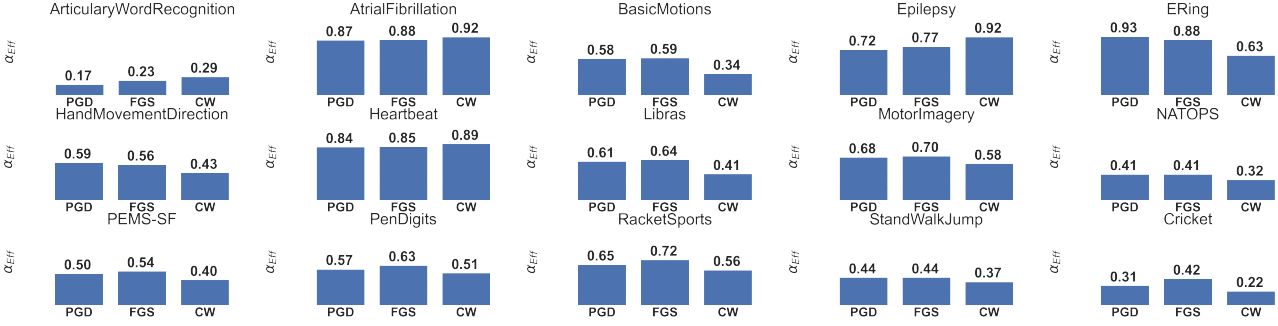


Fig. 27. Results for the effectiveness of adversarial examples from DTW-AR on different deep models using adversarial training baselines (PGD, FGS, CW) with l_1 -norm.

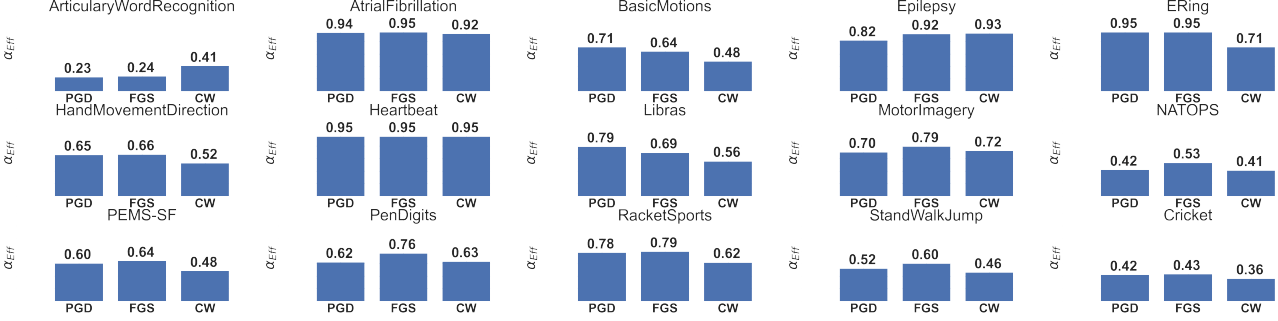


Fig. 28. Results for the effectiveness of adversarial examples from DTW-AR on different deep models using adversarial training baselines (PGD, FGS, CW) with l_∞ -norm.

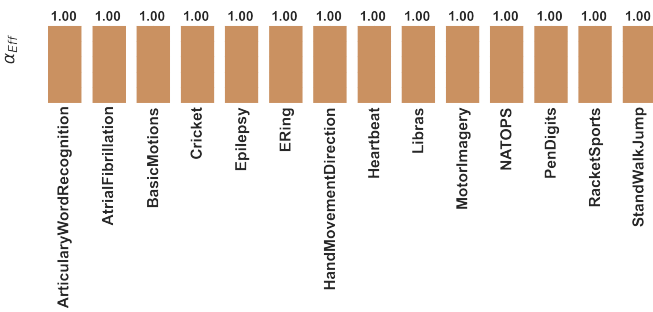


Fig. 29. Results of the success rate of DTW-AR adversarial trained model to predict the true label of adversarial attack generated from [31].

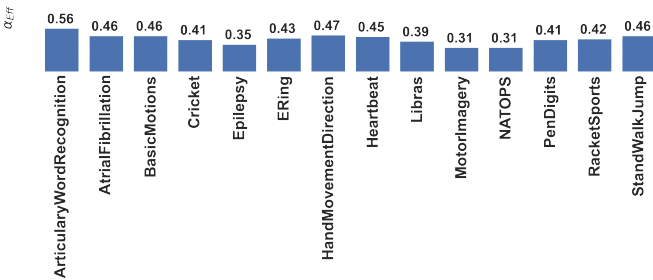


Fig. 30. Results for transferability of DTW-AR attacks across an LSTM model.

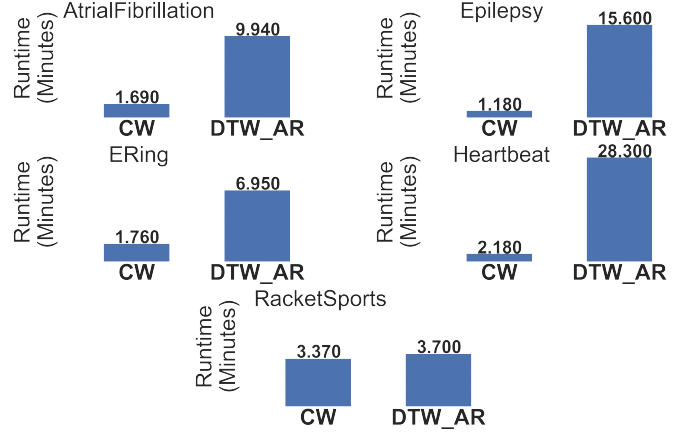


Fig. 31. Average runtime for CW and DTW-AR to create one targeted adversarial example (run on NVIDIA Titan Xp GPU).

APPENDIX C THEORETICAL PROOFS

C.1 Proof of Observation 1

Let l_2 be the equivalent of Euclidean distance using the cost matrix in the DTW space. $\forall X \in \mathbb{R}^{n \times T}$, there exists $\epsilon \in \mathbb{R}^{n \times T}$ and an alignment path P such that $\text{dist}_P(X, X + \epsilon) \leq \delta$ and $l_2(X, X + \epsilon) > \delta$.

The existence of ϵ is guaranteed as follows: We know from the nature of the DTW algorithm and the alignment paths that for two time-series signals X and X' , the optimal alignment path is not always the diagonal path. If ϵ does not exist, it means that for all signals X' that are different from

X , the diagonal path is an optimal alignment path, which is absurd. Thus, $\epsilon = X' - X$ and it always exists for any time-series signal.

Let P_{diag} be the diagonal alignment path in the cost matrix C .

For $X \in \mathbb{R}^{n \times T}$, let $\epsilon \in \mathbb{R}^{n \times T}$ such that the optimal alignment path P^* between X and $X + \epsilon$ is different than P_{diag} .

Let us suppose that there is no alignment path P between X and $X + \epsilon$ such that $dist_P(X, X + \epsilon) \leq \delta$ and $l_2(X, X + \epsilon) > \delta$. The last statement is equivalent to: $dist_P(X, X + \epsilon) < dist_{P_{diag}}(X, X + \epsilon)$.

Since we assumed that there is no alignment path P that satisfies this statement, this implies:

$$\begin{aligned} \forall P, dist_P(X, X + \epsilon) &\geq dist_{P_{diag}}(X, X + \epsilon) \\ \Rightarrow dist_{P^*}(X, X + \epsilon) &\geq dist_{P_{diag}}(X, X + \epsilon) \\ \Rightarrow DTW(X, X + \epsilon) &\geq dist_{P_{diag}}(X, X + \epsilon) \end{aligned}$$

Therefore, from the definition of $DTW(\cdot, \cdot)$ as a min operation during backtracing of the DP process, we get:

$$\Rightarrow DTW(X, X + \epsilon) = dist_{P_{diag}}(X, X + \epsilon)$$

Hence, $P_{diag} = P^*$, which contradicts our main assumption in constructing ϵ such that $P_{diag} \neq P^*$.

Therefore, we conclude that:

$$\exists P \text{ s.t. } dist_P(X, X + \epsilon) \leq \delta \text{ and } l_2(X, X + \epsilon) > \delta$$

C.2 Proof of Theorem 1

For a given input space $\mathbb{R}^{n \times T}$, a constrained DTW space for adversarial examples is a strict superset of a constrained euclidean space for adversarial examples. If $X \in \mathbb{R}^{n \times T}$:

$$\left\{ X_{adv} | DTW(X, X_{adv}) \leq \delta \right\} \supset \left\{ X_{adv} | \|X - X_{adv}\|_2^2 \leq \delta \right\} \quad (11)$$

We want to prove that a constrained DTW space allows more candidates adversarial examples than a constrained Euclidean space. Let $X \in \mathbb{R}^{n \times T}$ be an input time-series and X_{adv} denote a candidate adversarial example generated from X . In the DTW-space, this requires that $DTW(X, X_{adv}) \leq \delta$. In the Euclidean space, this requires that $\|X - X_{adv}\|_2^2 \leq \delta$, which is equivalent to $dist_{P_{diag}}(X, X_{adv}) \leq \delta$.

Suppose \mathcal{A} be the space of all candidate adversarial examples in DTW space $\{X_{adv} | DTW(X, X_{adv}) \leq \delta\}$ and \mathcal{B} be the space of all candidate adversarial examples in Euclidean space $\{X_{adv} | \|X - X_{adv}\|_2^2 \leq \delta\}$.

To prove $\mathcal{A} \supseteq \mathcal{B}$, we need to prove:

- 1) $\forall X_{adv} \in \mathcal{B} / X_{adv} \in \mathcal{A}$
- 2) $\exists X_{adv} / X_{adv} \in \mathcal{A} \text{ and } X_{adv} \notin \mathcal{B}$

Statement 1: Let $X_{adv} \in \mathcal{B}$. For the optimal alignment path P^* between X and X_{adv} , if:

- $P^* = P_{diag} \Rightarrow DTW(X, X_{adv}) = dist_{P_{diag}}(X, X_{adv}) \Rightarrow X_{adv} \in \mathcal{A}$
- $P^* \neq P_{diag} \Rightarrow$ According to Observation 1: $DTW(X, X + \epsilon) < dist_{P_{diag}}(X, X + \epsilon) \Rightarrow X_{adv} \in \mathcal{A}$

Hence, we have $\forall X_{adv} \in \mathcal{B} / X_{adv} \in \mathcal{A}$.

Statement 2: Let $X_{adv} \in \mathcal{A}$ such that $P^* \neq P_{diag}$. Consequently, according to Observation 1, $dist_{P_{diag}}(X, X + \epsilon) > DTW(X, X + \epsilon)$.

$$\Rightarrow dist_{P_{diag}}(X, X + \epsilon) > \delta.$$

As the diagonal path corresponds to the Euclidean distance, we conclude that $X_{adv} \notin \mathcal{B}$.

Hence, $\exists X_{adv} / X_{adv} \in \mathcal{A}$ and $X_{adv} \notin \mathcal{B}$.

C.3 Proof of Observation 2

Given any alignment path P and two multivariate time-series signals $X, Z \in \mathbb{R}^{n \times T}$. If we have $dist_P(X, Z) \leq \delta$, then $DTW(X, Z) \leq \delta$.

Let P any given alignment path and P^* be the optimal alignment path used for DTW measure along with the DTW cost matrix C . Let us suppose that $dist_P(X, Z) > DTW(X, Z)$.

We denote $P = \{(1, 1), \dots, (i, j), \dots, (T, T)\}$ and $P^* = \{(1, 1), \dots, (i^*, j^*), \dots, (T, T)\}$. Let us denote by k the index at which, P and P^* are not using the same cells anymore, and by l , the index where P and P^* meet again using the same cells until (T, T) in a continuous way. By definition, $k > 1$ and $l < \min(len(P), len(P^*))$. For example, if $P = \{(1, 1), (1, 2), (2, 2), (3, 3), (3, 4), (4, 5), (5, 5)\}$ and $P^* = \{(1, 1), (1, 2), (2, 3), (3, 4), (4, 4), (5, 5)\}$, then $k=3$ and $l=6$.

- If $k=l$, then $P=P^*$. Therefore, $dist_P(X, Z) > DTW(X, Z)$ is absurd.
- If $k \neq l$: To provide the $(k+1)^{th}$ element of P^* , we have $C_{(i_{k+1}^*, j_{k+1}^*)} = d(X_{i_{k+1}^*}, Z_{j_{k+1}^*}) + C_{(i_k^*, j_k^*)}$. To provide the $(k+1)^{th}$ element of P , we have $C_{(i_{k+1}, j_{k+1})} = d(X_{i_{k+1}}, Z_{j_{k+1}}) + C_{(i_k, j_k)}$. Using the definition of the optimal alignment path provided in Equation 1, we have $C_{(i_{k+1}^*, j_{k+1}^*)} \leq C_{(i_{k+1}, j_{k+1})}$. If we suppose that the remaining elements of P would lead to $dist_P(X, Z) < dist_{P^*}(X, Z)$, then this would lead to $C_{T,T} < DTW(X, Z)$, which contradicts the definition of DTW. Hence, we have $dist_P(X, Z) \leq dist_{P^*}(X, Z)$ implying that $dist_P(X, Z) > DTW(X, Z)$ is absurd.

Therefore, if we upper-bound $dist_P(X, Z)$ by δ for any given P , then we guarantee that $DTW(X, Z) \leq \delta$.

C.4 Proof of Theorem 2

For a given input space $\mathbb{R}^{n \times T}$ and a random alignment path P_{rand} , the resulting adversarial example X_{adv} from the minimization over $dist_{P_{rand}}(X, X_{adv})$ is equivalent to minimizing over $DTW(X, X_{adv})$. For any X_{adv} generated by DTW-AR using P_{rand} , we have:

$$\begin{cases} PathSim(P_{rand}, P_{DTW}) = 0 \text{ \& } \\ dist_{P_{rand}}(X, X_{adv}) = DTW(X, X_{adv}) \end{cases} \quad (12)$$

where P_{DTW} is the optimal alignment path found using DTW computation between X and X_{adv} .

Let P_{rand} be the random alignment path over which the algorithm would minimize $dist_{P_{rand}}(X, X_{adv})$. For the ease of notation, within this proof, we will refer to X_{adv} by X' .

We have $dist_{P_{rand}}(X, X') = \sum_{(i,j) \in P_{rand}} d(X_i, X'_j)$. As $\forall i, j, d(X_i, X'_j) \geq 0$, then minimizing $dist_{P_{rand}}(X, X')$ translates to minimizing each $d(X_i, X'_j)$.

Let us denote $\min d(X_i, X'_j)$ by $d_{\min}(X_i, X'_j)$, then $\min_{\text{dist}_{P_{\text{rand}}}}(X, X') = \sum_{(i,j) \in P_{\text{rand}}} d_{\min}(X_i, X'_j)$.

Using the back-tracing approach of DTW to define the optimal alignment path, we want to verify if $\text{PathSim}(P_{\text{rand}}, P_{\text{DTW}}) = 0$. Let P_{rand} be the sequence of cells $\{c_{k,l}\}$ and P_{DTW} be the sequence $\{c_{k',l'}\}$. Every cell $\{c_{k',l'}\}$ in P_{DTW} is defined to be the successor of one of the cells $\{c_{k'-1,l'}\}$, $\{c_{k',l'-1}\}$, $\{c_{k'-1,l'-1}\}$ which will make the distance sum along P_{DTW} until the cell $\{c_{k',l'}\}$ be the minimum distance. As we have minimized the distance over the path P_{rand} to be $d_{\min}(X_i, X'_j)$, the cells of P_{DTW} and P_{rand} will overlap. This is due to the recursive nature of DTW computation and the fact that the last cells in both sequences P_{DTW} and P_{rand} is the same (by the definition of DTW alignment algorithm).

Hence, $\forall (k, l) \in P_{\text{rand}}, (k', l') \in P_{\text{DTW}}$, we have $k = k'$ and $l = l'$.

Therefore, the optimal alignment between between X and X_{adv} will overlap with P_{rand} and we obtain $\text{PathSim}(P_{\text{rand}}, P_{\text{DTW}}) = 0$.

C.5 Proof of Corollary 1

Let P_1 and P_2 be two alignment paths such that $\text{PathSim}(P_1, P_2) > 0$. If X_{adv}^1 and X_{adv}^2 are the adversarial examples generated using DTW-AR from any given time-series X using paths P_1 and P_2 respectively such that $\text{DTW}(X, X_{\text{adv}}^1) = \delta$ and $\text{DTW}(X, X_{\text{adv}}^2) = \delta$, then X_{adv}^1 and X_{adv}^2 are not necessarily the same.

Let P_1 and P_2 be two alignment paths such that $\text{PathSim}(P_1, P_2) > 0$. We want to create an adversarial example from time-series signal X using one given alignment path. When using P_1 , we will obtain $X_{\text{adv},1}$ such that $\text{DTW}(X, X_{\text{adv},1}) = \delta$, and when using P_2 , we will obtain $X_{\text{adv},2}$ such that $\text{DTW}(X, X_{\text{adv},2}) = \delta$.

To show that $X_{\text{adv},1}$ and $X_{\text{adv},2}$ are more likely to be different, let us suppose that given P_1 and P_2 , we always have $X_{\text{adv},1} = X_{\text{adv},2}$.

Again, to simplify notations, let us notate $X_{\text{adv},1}$ by Z and $X_{\text{adv},2}$ by Z' for this proof. As we have $\text{DTW}(X, Z) = \text{DTW}(X, Z') = \delta$, then $\sum_{(i,j) \in P_1} d(X_i, Z_j) = \sum_{(i,j) \in P_2} d(X_i, Z'_j)$. If we suppose that by construction Z is always equal to Z' , this means that for $Z \neq Z'$, the statement $\sum_{(i,j) \in P_1} d(X_i, Z_j) = \sum_{(i,j) \in P_2} d(X_i, Z'_j)$ does not hold. The last claim is clearly incorrect. Let us suppose that Z is pre-defined and we assume $Z \neq Z'$. Let the ensemble of indices $\{k\}$ refer to the indices where $Z_k \neq Z'_k$. This means that we have $k - 1$ degrees of freedom to modify Z'_k to fix the equality $\sum_{(i,j) \in P_1} d(X_i, Z_j) = \sum_{(i,j) \in P_2} d(X_i, Z'_j)$.

Therefore, considering $\text{PathSim}(P_1, P_2) > 0$, we can construct $X_{\text{adv},1} \neq X_{\text{adv},2}$ such that $\text{DTW}(X, X_{\text{adv},1}) = \delta$ and $\text{DTW}(X, X_{\text{adv},2}) = \delta$.



Fig. 32. Results of DTW-AR based adversarial training to predict the true labels of adversarial examples generated by DTW-AR and the baseline attack methods on the Univariate dataset. The adversarial examples considered are those that successfully fooled DNNs that do not use adversarial training.